DISSERTATION

ON

INVESTIGATION OF BIOLOGICAL SAMPLE IN A NOVEL CRYO CHAMBER AT I-13 BEAMLINE IN DIAMOND LIGHT SOURCE (DLS)

Submitted in the Partial Fulfilment of the degree of

Masters of Research

In

Molecular Modelling and Materials Science

Department of Chemistry

University College London, UK

August 26, 2016

Name- Archana Bhartiya

Supervisors- Prof Ian K Robinson and Dr Mohammed Yusuf

*Placement Organization- **R**esearch **C**omplex at **H**arwell (RCaH).*

Subject- Advanced Research Project (CHEMGM01)

ACKNOWLEDGEMENT

In the completion of the present dissertation, there are feelings of achievement and satisfaction. In these moments of happiness, I take the opportunity to record my sincere gratitude to all those who mattered.

First of all, I would like to express my prayers to the almighty God-Lord Shiva for his abandon blessings, mercy and grace that he showed upon me.

I also take opportunity to express my sincere thanks to my academic supervisor Prof Ian K Robinson and my second supervisor Dr Mohammed Yusuf for their worthy cooperation, noble guidance, constructive criticism, innovative ideas, valuable suggestions, and unending inspiration. I would also like to thanks Research Complex at Harwell and I-13 beamline, Diamond Light Source for giving me opportunity to perform all practical and opportunity to do X-ray imaging at I-13 beamline. I also appreciate support of Dr Fucai Zhang for sharing his valuable reconstruction images, Dr Majid Abyaneh for giving sample holder and Fernando-cacho-nerin for providing his cryo- equipment during beam time. I am also grateful to Xiaowen Shi and Mathieu Calvat for helping me during beam time at I-13 in setting up the beamline.

It also gives me great pleasure to thank Dr Zhimei Du, Dr Chris Blackman and Prof Ivan P Parkin, Department of Chemistry, University College London UK for their useful guidance in every way throughout my academic year.

My efforts will remain incomplete if I don't express my love and deep gratitude to my parents for their never ending affection and untiring efforts for bringing my dreams and ambitions to a proper shape.

Last but not the least I would like to thank various organizations for supporting my research for 4 years they are listed below-

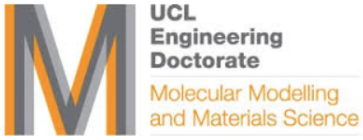

ABSTRACT

Dissertation reflects the size, volume, morphology of the rabbit red blood cells in different osmotic pressure (Isotonic, Hypotonic and Hypertonic in NaCl salt solutions) fixed with glutaraldehyde chemical observed under confocal microscope and confocal images were processed by Image J software for analysis. The goal was to prepare biological samples with the plunge freezing method, and transfer the sample into the beam line I-13 coherence branch (DLS) vacuum chamber without crystallization of the water content which is built by Prof Robinson's group. The biological samples are then imaged using the X-ray ptychography technique, which requires numerical reconstruction of a set of diffraction patterns with spatial resolution of >50nm. The novel vitrified (cryo) sample with combination with ptychography phase retrieval algorithms- high resolution imaging technique, is excellent method for imaging biological sample at nanometer scale, close to their native state by plunge freezing or chemical fixation (glutaraldehyde) has future prospective in studying diseases occurring due to morphology change of cells. This report also shows difference in morphology of RBCs with and without glutaraldehyde fixed samples and gives outline of sample before and after X-ray beam hits in order to compare ice formation and radiation damage to the samples. 7.5KeV energy used which falls under hard x-ray generated from synchrotron.

Keyword: Osmotic Pressure, Rabbit Red Blood Cells, Ptychography, Glutaraldehyde, Plunge Freezing, NaCl salt concentrations, I-13 Beamline, Ice Formation and Radiation Damage.

TABLE OF CONTENTS

1. INTRODUCTION

Blood is continuously flowing fluid present in organisms responsible for transport of oxygen from lungs to all parts of the body and removes carbon dioxide as a waste. Flow rate of blood regulates body temperature and pH to keep running normal metabolism of organisms. Blood is blend of various other components such as **R**ed **B**lood **C**ells (RBCs, red colour, 45%), plasma (yellowish, 55%), **W**hite **B**lood **C**ells (WBCs, white colour, <1%), platelets (colourless, <1%), salt, ions and protein (1). It is commonly known as erythrocytes which produces from bone marrow at a rate of about 2-3 million cells per second. RBCs are in different shape when they are produced and once they fully mature, acquires biconcave disc like shape which contains protein known as **H**emoglobin (Hb) that makes RBCs red in colour, biconcave shape is due to absence of nucleus and mitochondria (2), it drives its energy from **A**denosine **T**ri-**p**hosphate (ATP) (3), which is generated from glycolysis metabolism in cytoplasm. To have ability to reform makes it flow through small blood capillaries of body without any jerk.

Various major components of blood have specific importance- red blood cells is to carry oxygen all over the body for metabolism from lungs, also transport nutrients, hormones and removes waste product through various means such as liver, kidney and intestine. WBCs protect from infectious disease and foreign invaders blood platelets protects from excess bleeding by clotting quickly at damaged area of blood vessels and finally salt, cations, anion and protein maintains the temperature, pH and osmotic pressure of the cells (1).

Hundreds of Hb molecules present in each RBCs to carry oxygen and it is nearly spherical with diameter of 55Å. Hemoglobin is tetramer protein with 2 alpha and 2 Beta subunits of average 145 amino acid and each subunit have one iron atom centralized by porphyrin ring and together known as heme group, the unique cooperativity behavior of hemoglobin allows binding of oxygen to the hemoglobin (4). There are four iron atom among10,000 other atoms along with protoprophyrin that form 4 heme group of hemoglobin which was analyzed using x-rays by Max pertuz. RBCs has ability to command its volume which represents amount of hemoglobin present in cell and concentration of cation present regulates the exchange of sodium and potassium level in cell membrane plus maintains the viscosity of cytoplasm.

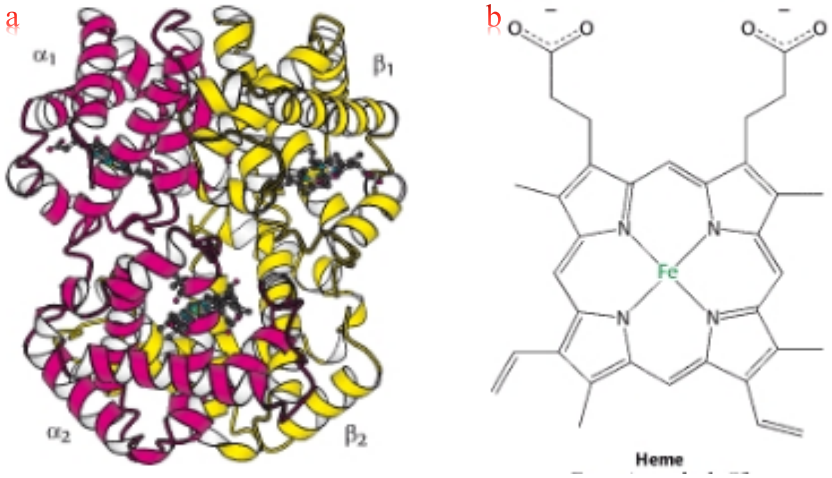

Figure 1 Quaternary structure of hemoglobin a) Four subunits-two alpha and two beta chain of hemoglobin and each one consist of b) Fe-protoporphyrin ring called heme (5).

It is made up of 2 identical alpha-helix and 2 identical beta-sheet opposite to each other (Fig 1a) which combines to form quaternary structure with non-polar interactions and hydrogen bond. The iron atom in heme binds to the four nitrogen in the center of protoporphyrin ring (Fig 1b). Hemoglobin when combines with oxygen are in relaxed state (R-state) end up into planar configuration known as oxygenated blood and without oxygen it is in tight state (T-state) leads to domed configuration known as deoxygenated blood (4).

1.1 Why Choose Rabbit Red Blood Cells?

Species	Diameter (um)	Volume(um^3)	Life Span
Human	7.3	95	120 days
Rabbit	6.1	76	57
Pig	5.81	61	-
Mouse	5.8	41	-

Table 1 Table shows the difference of diameter, volume and life span of RBCs of different species (6).

Rabbit red blood cells is genetically and morphologically similar to human RBCs (Table1), so it could be used to identify genetic mutant disease for human welfare and also blood flow regime is also similar to human, less pathogenic and hazards to work in laboratory. The volume and diameter of rabbit RBCS is more close to human than other animal mention above table 1. It has some

experimental advantages such as immune response, pathology to test disease and infection which corresponds to human, it's also used for diagnosis human disease caused by mutation, for example neoplasia disease caused due to mutation in one of rabbit gene (6). "Rabbit blood is one of the animal models which most closely resembles human blood and is crucial for cancer research" according to famous blood selling company Fitzgerald (7).

1.2 Diseases Related to Red Blood Cells

There various disease which is caused due to change in the shape of RBCs affected by osmotic regulation, mechanical stress, pH and chemical agents present in the blood (8). Radiation damage also mutate the cells and affects the conformation of proteins and lipid membrane of cells which eventually leads to severe consequences of diseases (9) and also reduces the cell count during treatment of cancer patients from constant radiation therapy. Ageing and dehydration of cell are some common type of disease which cause due to cell deterioration and ability to control cation homeostasis respectively that leads to lose of hemoglobin number and eventually volume and surface area of RBCs decreased. Most common example is sickle cell anaemia (cause due to creation of RBCs), parasitic disease like malaria, hereditary sperocytosis and hereditary elliptocytosis are type of disease which is caused by change of RBCs shape from biconcave to small circular and oval shape affected RBCs respectively and reduces its deformability ability which will hinder while flowing through micrometer size blood vessel (3).

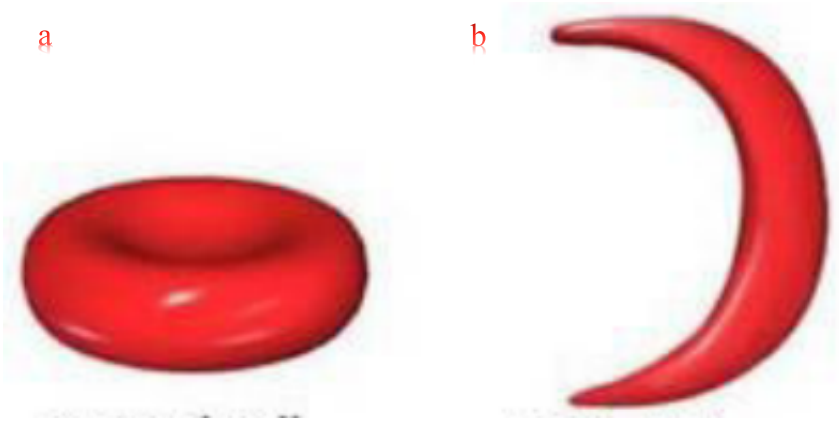

Figure 2 Red blood cells a) normal biconcave disc shape cell b) sickle cell affected cells (10).

Healthy RBCs are diciod shape with ability to become oxygenated & deoxygenated cells in presence & absence of oxygen respectively whereas unhealthy cells tends to have C-shaped from which sickle cell name rises, crises of blood cells in plasma leads to vaso-occulsion because cells lives for shorter time compared to healthy cells which consequently leads to fatigue, anemia, body pain, organ damaged and eventually death of affected people in severe condition of blockage of blood cells

because of C-shaped of cells and this shape change occurs due to "substitution of amino acid coding for Beta-globuin subunits" also it loose ability to carry oxygen and retain deform shaped (11). This disease was first reported by James perrik, 1910 in a west Indian student (12) from their it become important to study structure and morphology of RBS.

1.3 Osmosis- Hypertonic, Hypotonic and Isotonic Condition

Osmosis is process of transport of solvent from higher concentration to lower concentration through semi-permeable membrane, this process regulates and maintains the level of cation, anion, minerals and nutrients in blood of every organism.

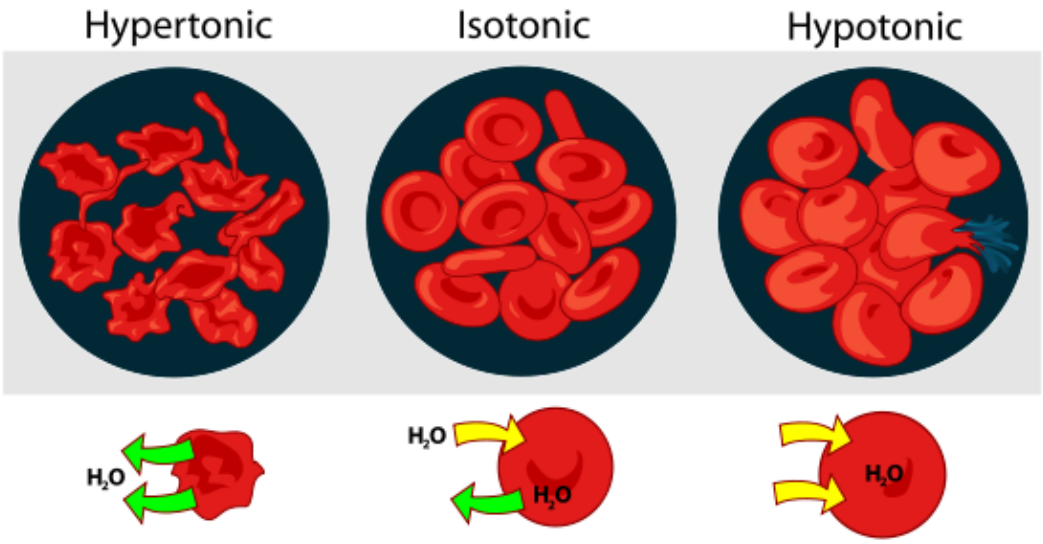

Figure 3 Red blood Cells showing three major conditions of osmosis in addition to fluctuation of water content inside cells; outgoing water -Hypertonic, equilibrium -Isotonic and intake of water -Hypotonic by cells (13).

There are three osmotic conditions such as Isotonic (normal cell): It means intake and outgoing of H_2O from the cell is in equilibrium. Hypertonic (shriveled cells): loss of water from the cell due to higher concentration of H_2O inside the cell and Hypotonic (swollen cells) intake of water due to low concentration of water inside cell. Osmotic fragility test proves that hypotonic concentration of **S**odium **C**hloride (NaCl) is consequences to lysis of cells (14).

Hypotonic solution makes cell membrane porous of 3nm diameter by lysenin (15) and develop channels of 30A by iturin chemical (16) which leads to hemolysis of blood cells. It is hard to measure the preceding stage of cell membrane before the hemolysis because it so fragile and does not last for long time in mechanical or chemical stress (17). Hyper osmotic solution is functional fluidic therapy to trauma patient to restore "blood volume" and "mean arterial pressure" from haemorrhage, its shrinks the cells and decrease the cell volume from swollen cells (18).

1.4 Shapes of Red Blood Cells

Normal healthy human RBCs is discocyte shape with average diameter of 7- 8 µm and thickness of 1- 2 µm, "the membrane of the RBC comprises a phospholipid bilayer and an underlying two-dimensional network of spectrin molecules" which protects from any stress/damage, regulates the permeability rate and also provides unique elastic property to pass through 2-3 µm diameter blood vessels (3), the density of spectrin network and presence of ATP content regulates the shape of RBCs (8) by monitoring the interactions of spectrin network and phospholipid bilayer (19). At shortage of oxygen both rabbit and human RBCs stimulates ATP which can control vascular system and widens the skeletal muscle to meet the need of metabolism (20).

1.5 Known Microscopy Methods for Imaging

Very common microscopy methods used for imaging biological samples are light microscope, **T**ransmission **E**lectron **M**icroscopy (TEM), **S**canning **E**lectron **M**icroscopy (SEM) and optical microscope. Some analytical techniques such as **S**canning **T**ransmission **E**lectron **M**icroscopy (STEM) which uses electron beam to scan the sample (21), it also has ability to image frozen-hydrated and thick biological samples <300nm (22) from structural analysis to molecular and to elemental stage of biological sample. **S**econdary **I**on **B**eam **I**maging (SIBI) is considered as most powerful technique for analysis of elemental information and chemical composition of biological samples with association of **E**nergy-**F**iltered **T**ransmission **E**lectron **M**icroscope (EFTEM) and TEM ability for better contrast (23). Affinity of cell membrane of red blood cells can be studied using **A**tomic **F**orce **M**icroscopy (AFM) at growth stage of cells, it determines how strongly the lipid membrane are bound to the cells plus it also help to distinguish mixed layer of A and O blood group from its contrast image representation by AFM (24). Hydrophobic nature of **R**aman **S**pectroscopy (RS) makes its suitable for imaging biological samples such as red blood cells infected with malaria parasite, it helped to visualize the early stage of infection at a molecular level (25). **O**ptical **M**icroscopy (OM) is used to study dynamic and mechanical stress done on the live RBCs, using quantitative phase contrast imaging method at cellular to sub-cellular level (26). The Light microscope has also important role in cell biology to study structure of proteins, cell organelles and various tissue using corresponding fluorescent dyes at cellular level resolution (27). The above mention microscopy methods are good with only some particular parameters required for imaging such as spatial resolution, sample thickness, image contrast, time consumption and sample size, neither of them fulfil biological sample imaging requirements, so x-rays come into action which are electromagnetic wave falls under in electromagnetic spectrum to make possible to image biological samples at their native state along with all other parameters because it has high penetrating power and ability to provide better contrast image of biological sample at sub-cellular levels.

There are also some different technical limitations and resolution issues with other conventional light and electron microscope used for biological samples. X-rays microscope solves the problem by analyzing the sample at high resolution and with less technical issues plus imaging atomic to molecular level details of materials and also it does not require sample processing such as fixing, staining and sectioning -it can image thick samples also (28).

X-rays falls under electromagnetic radiations that travels with speed of light and originate from radioactive element producing specific range of photons that ionize the materials and gives atomic level of information of materials and biological specimen. There are 2 types of x-rays depending upon there penetrating power known as soft x-rays and hard x-rays (29) for imaging most of the biological sample at micro-level and also to study structural and morphological details of the various biological samples.

1.6 Soft x-ray Imaging

Soft x-rays are advantageous over other conventional methods because it protects from sample mass loss plus avoid morphological distortion of sample even at radiation dose of 10^{10} Gray (1Gy=1J/Kg) and can also image frozen hydrated biological samples in parallel maintains structure close to its native state (30). Soft x- ray produce energy <10KeV (31), it has longer wavelength, low penetrating power and energy thus suitable for less dense substance such as studying agricultural and food products (29). Soft x-ray causes less radiation damage to the formalin fixed sample (32). "Soft x-rays operates in the 'water window' of spectral region between the carbon k-edge at 284eV and the oxygen k-edge at 540eV" (30) which means that soft x-rays is efficient in emitting electron from K-shell of carbon and oxygen atoms of a sample containing water and gives high resolution imaging.

1.7 Hard x-ray Imaging

Hard x-ray is "lensless" microscope with ability to collect far field diffraction pattern of internal and external structure of biological specimen and it uses fast calculation method of iterative algorithm to reconstruct diffraction pattern obtained to produce good quality image (33). Hard x-rays generated from SR source has wide application for studying structural information of biological samples and atomic level information of materials (34) Hard x- rays produce energy range 25 -200KeV (35), hard x-rays have shorter wavelength, high penetrating power and energy thus used for studying cellular and sub-cellular structure of biological specimens and further used in medical diagnosis (29). Hard x-ray is significant for thick biological sample (chromosomes) because of its high penetrating power and high spatial-resolution imaging ability. Efficient properties of hard x-rays such as low absorption, scattering, faster scanning and refraction of beam after hitting the samples can be used to recognize damaged part of tissue furthermore applied in clinical application to treat patients, it also used to

diagnose fracture bone of human in hospital (36). Hard x-rays can be obtained imaging resolution of ≥10 nm which can be further improve by using multilayer zone plate. Various lens used for focusing x-ray beam but **C**ompound **R**efractive **L**ens (CRL) is efficient concave lens for focusing hard x-rays beam that let to adjust other parameter such as focal length, spot size and focal distance and number of CRL used in focusing depend upon the energy of beam (37).

1.8 Synchrotron- Third Generation Energy Source

Synchrotron **R**adiation (SR) generated by bunch of charged electrons accelerating in a circular ring within GeV energy producing electromagnetic spectrum range, specially characterize under hard x-rays and soft x-rays, synchrotron is the third generation energy storage ring with lower emittance and with high power periodic magnets which deflects and bends charged electron to produce reasonable brightness and "considerable degree of spatial coherence" (38). In Diamond Light Source (DLS) synchrotron facility, UK- the electron injected into a Linec accelerator where electron accelerates with energy of 10Mev in a circumference of 158m and then after its transferred to circular ring of 561.6m circumference where electron accelerates at 3GeV of energy and produce photons range of 4-20 KeV, eventually shoots to 24 sector with the help of powerful magnets for research in different field, the longest beam line of SR source is I-13 Imaging and coherence branch with 250m long (39). Undulators and wigglers are two types of magnetic devices jointly known as **I**nsertion **D**evices (ID), former used for collimating beam horizontally and vertically and later is used to produces "continuous spectrum with higher flux" gradually to shorter wavelength before beam bends (38).

Synchrotron is novel approach to study ultrastructural information of hydrated cells at resolving power of 30-50nm, sample preparation method is less laborious as it does not need chemical staining and heavy metal fixation for better contrast (40). It makes possible to image thick biological sample (chromosomes, RBCs etc) in their native state at high resolution after its been plunge frozen which furthermore protects from sample from radiation damage (41).

Synchrotron has vast number of importance in biology and drug development such as resolving physiological and pathological aspect of plants, animals and human, for example understanding the function along with development of **C**entral **N**ervous **S**ystem (CNS) of human and animal (42), Zhang et al managed to visualize micrometer level of information of "cerebral angioarchitechture" using **S**ynchrotron **R**adiation **P**hase **C**ontrast **I**maging (SR-PCI) technique (43). It also has clinical application by using SR with radiotherapy to treat cancer patients, SR is also used to study metallurgy and chemistry of different proteins (> 80% of proteins), stored in **P**rotein **D**ata **B**ank (PDB) with their structural and molecular level of information (42).

1.9 IMAGING TECHNIQUES

1.9.1 Coherent X-ray Diffraction Imaging (CXDI)

Interference is the basic property of coherent beam. Coherent x-rays imaging technique is a "lensless" method which means it uses computer algorithm instead of lens unlike conventional microscope for imaging non-periodic nanoparticles, nanocrystals, extended biological and material science samples to visualize 2D and 3D structure with using phase-retrievel algorithm in order to obtained better contrast imaging (44). CXDI can image thick biological sample with high resolution contrast, various optics present to make the beam more focus such as Fresnel zone plate and **C**ompound **R**efractive **L**enses (CRL) (45). There are four types of CDI methods for studying internal and external structure of samples by collecting far field diffraction of the object such as plane wave CDI (Fixed sample illumination), Ptychography CDI (diffraction of non-periodic substance with fixed illumination), Bragg CDI (structure of nanocrystal) and Fresnel zone plate CDI (to produced curved wave front focus sample (46).

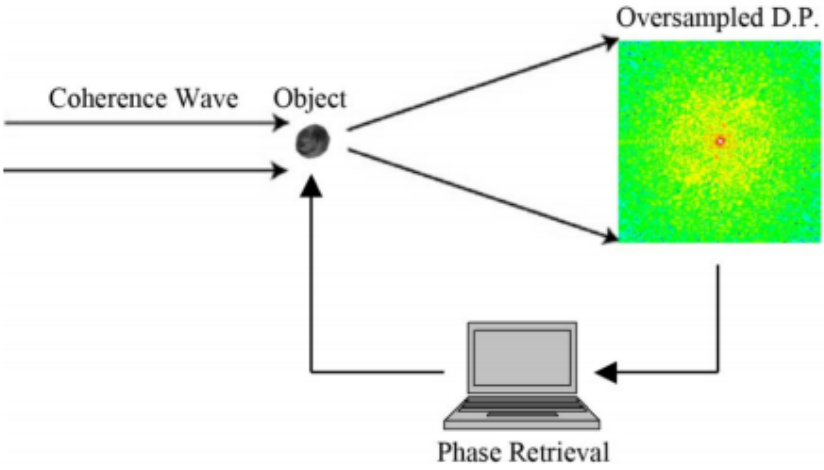

Figure 4 Principle of CDI where a coherent wave illuminates an object and the oversampled diffraction pattern is measured by an area detector. An image is reconstructed from the diffraction pattern by using an iterative algorithm (46).

Oversampling solve the phase problem of 2D and 3D reconstructions by increasing the magnitude of Fourier transform by factor of 2X (47). In diffractive imaging partial spatial coherence gives less artefacts in reconstruction than full spatial coherence of the illumination beam(48). Oversampling of the object is taken into account by calculating distance between detector and sample, sample thickness, aperature size, pixel size and wavelength of incident beam to calculate the diffraction pattern of object (46).

CDI also has other application such as X-ray -Free Electron Laser (XFEL) where pulse rate is 10 femtosecond (fs) for imaging biological sample nevertheless it has disadvantage of sample damage,

CDI also has application in single particle imaging, single particle of a molecule is challenging experiment for to be performed (46).

Nishino et al, 2009 made an attempt to image 3D structure of human chromosomes using CDI and synchrotron energy source, diffraction pattern obtained to reconstruct into image by iterative algorithm but unfortunately no internal structure detail was resolved after reconstruction, which shows that hydrated sample can be scan to their native state without any chemical stain fixation (34).

1.9.2 Ptychography- Technique for Reconstructions

A scanning coherent diffractive imaging (CDI) technique in which object illuminated and scanned in a step-wise fashion, resulting in an array of partially overlapped probe spot on the object; obtained diffraction pattern from each spot recorded and later complex inverse FFT algorithms is used for reconstruction of diffraction pattern into images (49).

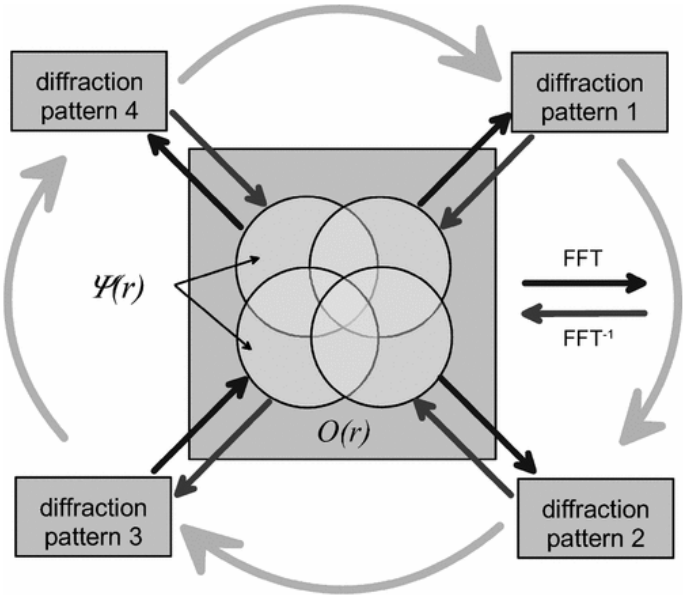

Figure 5 Phase retrieval algorithm for reconstruction of diffraction pattern (33).

Ptychography coherent x-ray imaging is introduced to solve the phase problem of CDI by introducing scanning pinhole before the sample which rotates 360 degree and illuminate object at different angle to capture each position in order to produce close to native structure of the sample (50). It has advantage of both high penetration power of hard x-rays and high sensitivity of lensless CDI (51), which means it has potential for qualitative imaging at high resolution from collected datasets and reduces the loss of information from the sample.

Many samples imaged using coherent diffraction such as freeze-dried diatoms at resolution of 30nm, bacteria at 20nm resolution, frozen-hydrated yeast at 85nm resolution and also 3D nonporous glass at resolution of 30nm and it also has various application in research of biological material area (90).

It corresponds to Nyqvist-Shannon Theorem of oversampling (52) because it takes stepwise images of same object and combines the data to produce good quality of image.

Reconstruction into image is also an important step form diffraction pattern, to retrieve frame by frame information of an object by using available computer algorithms such as **P**hytological **I**terative **E**ngine (PIE) is one of them to solve phase problem but its drawback of constant illumination of wave front to object gave birth to extended Phytological Iterative Engine (ePIE) algorithms which considered both object function and complex illumination (probes) function (50). In ePIE, Fourier transform wave front incident on sample to obtained diffraction pattern which later process by inverse Fourier transform to reconstruct into images to produce high resolution image with decreased signal to noise ratio (50). This algorithm helps to solve phase problem unlike other algorithm such as swrink wrap technique which contraints the image and give better resolutions.

For good reconstruction of image certain parameter should be set priori such as illumination probe function and translation steps, former should be smaller than later to obtain good diffraction pattern of overlapped sample position; Zhang et al propose that Ptychography can be used for both short and long wavelengths but some limitation can hinder like system instability and inaccuracy for short wavelength sensitivity and misalignment for long wavelength (53).

1.9.2 Radiation Dose- Major Problem of X-rays

Radiation damage to all sort of specimen due to x-rays radiations is supreme issue and it defines as amount of ionizing energy absorbed per unit mass by the sample. Things to be considered while measuring radiation dose is sensitivity of detector, optimizing radiation dose by calculating intensity of beam at certain seconds of interval before it reaches to the sample and of course thickness of sample because thick sample are less likely to get damaged. Radiation damage resolution for 3D diffraction image can be calculated by considering two points i) “required dose by imaging” and ii) “maximum tolerable dose” by sample and quantitative image obtained only when given dose is greater than required dose and less than maximum tolerance dose (54).

Soft x-rays disrupt intact chromosomes structure by 10-100nm resolution at frequency range of 10^4-10^7Gy, resulting the double strand of **D**eoxyribose **N**ucleic **A**cids (DNA) completely breaks and losses it’s morphology. According to Malcolm et al paper the scaling law for required dose should be one upon fourth power of resolution ($1/d^4$) and 1nm sample can observe 1.0×10^8 Gy radiation dose and they are limited to 10nm thickness of frozen hydrated sample (54). Calculation of damage should be performed prior to the experiments and after the experiments to calculate absolute information gained from diffraction patterns plus radiation damage occurring between sample and detector should also be considered seriously(55).

1.10 Difference between Chemical fixation and Cryo fixation

Biological samples are difficult to measure because water content level in cells is more and if they dehydrated they lose their structural conformation, so to prevent dehydration samples are chemically fixed and frozen to reduces dehydration. There are various methods for fixing biological sample such as chemical fixation (gultaraldehyde, osmium tetraoxide, platinum blue, uranyl acetate), dehydration by ethanol/acetone/methanol, embedding by epoxy resin and cryopreservation (High pressure plunge freezing, propane jet freezing and slam freezing) (56). Chemical fixation and dehydration is instant method for fixing sample to visualize under **T**ransmission **E**lectron **M**icroscope (TEM)/**S**canning **E**lectron **M**icroscope (SEM)/X-rays and to increase the contrast by electron absorption in TEM/SEM (57) but they have negative effects as they don't give exact structural information due to cross linking of proteins by diffusion/osmosis through permeable membrane furthermore it gives less dense image compared to original cells/tissues and it also distorts the structure due to harsh chemical chemistry. In resin embedding fixation, the most embedding resin polymerize at 60-70 °C and become hard plastic resin which further trimmed to trapezoid shape and later sliced into thin sections by glass/diamond knives, ultrathin sections collected into small water reservoir eventually scope by copper grids for imaging under microscope and this technique is used for studying morphology of biological samples (58).

Most reliable technique is plunge freezing which is widely used by many scientists/researchers to study molecular level to atomic level of information of biological specimen.

Aqueous biological high pressure plunge freezing maintains the native state of biological samples for imaging methods such as cryo TEM and cryo X-rays (59). In plunge freezing samples get vitrified in liquid nitrogen and become amorphous while plunging. Samples are stored in liquid nitrogen after plunge freezing at very low temperature. The advantages of plunge freezing are that it preserves the sample and gives high resolution images with less radiation damage but negative part of this procedure is that sample needs to be stained to get better contrast because untrained sample does not show good contrast and it's also limited to depth freezing.

1.11 X-ray Experiment Done on Red Blood Cells

Several experiment done on RBCs by synchrotron energy source, one of example is observing stepwise aggregation of human RBCs in different solution such as plasma, PBS and **P**oly**V**inyl**P**yrrolidone (PVP) and result was concluded by analyzing the speckle size and contrast which alters with increasing aggregation of RBC eventually it was predicted that RBCs in PBS are bigger in size plus high contrast speckle pattern obtained and this was study done by "x-ray phase contrast imaging" method (60).

2. Material and Methods

2.1 Red Blood Cells

Red blood cells were ordered commercially from Innovative Research (Catalog No.: IC10-0510) which was pre-extracted from New Zealand White Rabbit and later been washed (free from plasma, white blood cells and other traces present in blood) and re-suspended in small amount of alsevers solution for preservation plus to prevent coagulation. Commercially Filtered RBCs was collected and stored at 2-8°C until it is to be used and it work best within 28 days after withdraw.

2.2 Transmission Electron Microscope (TEM) Grids

Two types of 3mm diameter TEM grids were used during experiment i) carbon film grids (Taab-Laboratory and Microscope) - circular copper grids bars with of 400 mesh of 7um x 7 um square array with spacing of 250um and coated with thin film of carbon, it has two sides shiny and dark-shiny side is more suitable for sample and ii) Silicon nitride wafers (Silson Ltd.)- it is structured as 0.25mm x 0.25mm square silicon nitride window at the centre with window thickness of 30nm which is supported by octagonal silicon frame of thickness 200µm, this also has flat and non-flat surface window-flat surface is more suitable for sample. Both grids are suitable to mount into standard TEM holder.

2.3 Hydrophilic Grids

We opted two methods for making grids hydrophilic i) Grids soaked in 10% Poly-L-sine solution (1:10 dilution, Boster) (900µl of milliQ water plus 100µl of Poly-L-sine for 1ml solution) for 30 mins to coat monolayer of poly-L-sine and make grids hydrophilic, after 30 mins grids were taken out carefully using fine tweezer and placed on slide wrapped with parafilm for another 20 mins, left it to dry and then finally ready to use ii) Grids were placed on parafilm wrapped slide, kept inside the evacuated chamber connected with power supply using Quorum glow discharge equipment, adjusted up to pressure of 2 bar and treated with plasma (electric created by air) for 15sec to make grids hydrophilic and negatively charged to adhere positively charged RBCs.

2.4 NaCl Preparation Method

Prepared various concentrations of sodium chloride (NaCl) salt such as 0.9%- Isotonic solution (0.45g in 50ml of milliQ water, pH-7.13), 0.6%- Hypertonic solution (0.15gm in 25ml of milliQ water, pH-6.90), 10%- Hypertonic solution (2.5gm in 25ml of milliQ water, pH-6.80). Required pH adjusted by calibrating acidic and basic concentration of a solution before use.

Method: Taken respective volume (50ml and 25ml) of milliQ water in falcon tube and weigh appropriate amount of NaCl salt mentioned above carefully using weighing balance and dissolve in milliQ water vigorously eventually pH of solution adjusted according to requirement.

2.5 Sample Preparation

Pipette 1 ml of each salt concentration solutions into labelled eppendorfs (A), add 20µl of rabbit red blood cells in appropriate solution and mix well using vortex, dilute the sample (A) further with ratio of 950µl of salt solution (Isotonic, Hypertonic and Hypotonic respectively) plus 50µl of sample labelled (A) into new eppendrof labelled (B). Centrifuge sample (B) at 10rpm for 10 mins- discarded supernatant and used pellet; to fix the cells it was treated with 8% glutaraldehyde (diluted to 2.5% into distil water). 5 µl of sample (B) smeared on slide and covered with coverslip and lastly observed under confocal microscope to check the density of the sample and later in order to acquire appropriate density, cells were observed under confocal microscopes for which 3µl of sample pipette on hydrophilic silicon nitride window and copper film grid.

2.6 Sample Transfer Method

Used screw mechanism TEM sample holder of 10mm diameter (borrowed from IO8 beamline, DLS); for mounting the sample onto sample holder and then into cryo chamber. Holder is unscrewed and sample grid is mounted into the holder carefully using very fine tweezers with expertise and tighten the screw of the holder using little screw driver eventually carried to I13 beam line **D**iamond **L**ight **S**ource (DLS) and mounted onto the copper base inside the cryo chamber located inside I13 hutch.

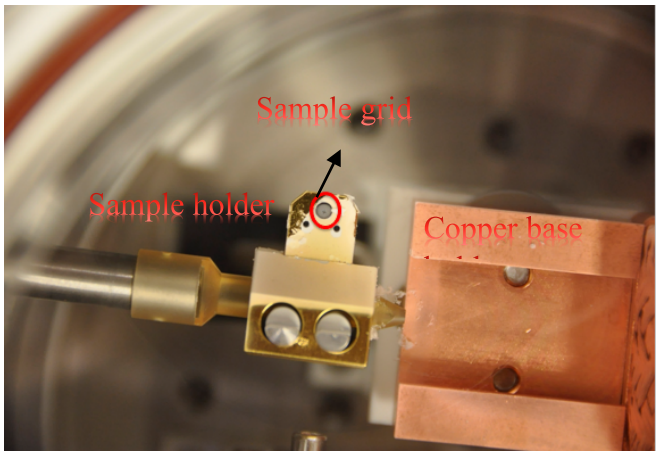

Figure 6 Brass sample holder with copper base to attach sample holder containing sample grid into the cryo vacuum chamber

In the setup used here the holder carrying sample is attached to a copper plate which slots into a copper sample holder. This part is mounted on a piezo-actuator translation stage and to keep thermally isolated silica balls and aluminium is used.

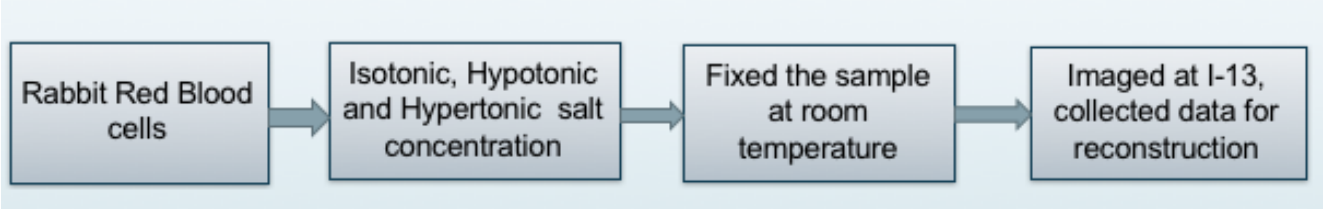

Figure 7 Schematic diagram of Red Blood Cells sample preparation.

2.7 Confocal Microscope

Efficient combination of Olympus OLS4100 confocal laser scanning microscope and Lext software program used to get coloured and laser 2D-3D image of red blood cells after scanning. High magnification of 5x and 10x lenses were used for localization of cells and 20x and 50x lenses used for taking image of the sample for validation, so that it can be send for X-ray imaging. Measurement tool used to measure the length of the cells and compare the size difference of the cells under different osmotic conditions.

2.8 Plunge Freezing

Samples were plunge frozen in 2 different conditions (3ul sample on grid and blotted for 0.9s, 4ul sample and blotted for 1s inside Leica system); humidity of Leica should be maintained at 100 degree while plunging. Hydrophilic grids (Silicon nitride and 7um x 7um copper grids) were held with fine tweezer and attached inside the Leica, furthermore, 3ul and 4ul of sample were dropped on grids and brought to plunger (Leica), where it blotted for 0.9-1.0 second by blotting paper, straight after blotting the plunger dropped the sample into a cryogen tank, containing liquid nitrogen and liquid ethane, once the grid enters the liquid ethane, the sample is rapidly frozen and gets vitrified and stored in blue cryo holder- for short storage. Same procedure was repeated with all grids. Plunge frozen samples were stored in liquid nitrogen dewar for later use.

2.9 ImageJ Software

ImageJ is a free software for processing many biological images. Imaged took from confocal microscope, saved in Tiff format were then analyzed in ImageJ software to measure the length, volume and counting number of cells present on the TEM grids and processed imaged save in Jpeg format and select measure from Analyze tool from the bar to obtain results.

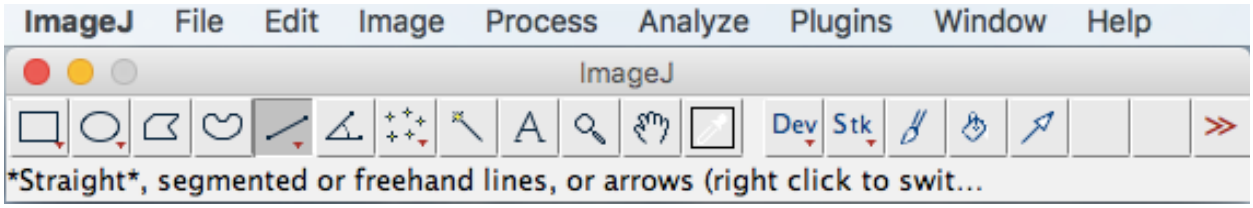

Figure 8 Figure of ImageJ software table for calculating length of the cells

a	Area	Mean	StdDev	Angle	Circ.	AR	Round	Solidity	Length
1	2.402	65497.167	3.869	-90	1	0	0	NaN	3.164
2	5.604	65457.107	9.692	-63.435	0.977	0	0	NaN	8.489
3	1.601	65474.25	2.63	-90	1	0	0	NaN	1.898
4	4.804	65485.371	7.108	-100.305	1	0	0	NaN	7.074

Slice b	Count	Total Area	Average Size	%Area	Mean	Circ.	Solidity
0.9%_50x2.tif	370	4657.339	12.587	5.735	255	0.773	0.838

Table 2 RBCs in 164mM NaCl marked in purple **a)** Outcome table of length & area calculated by software of each cells **b)** ImageJ summary table of number of counts and circularity of RBCs.

For counting number of RBCs, confocal images are converted into grey scale> reduced background noise>set appropriate threshold>watershed-separate different cells by one pixel>Analyze particle for counting each cells present on the grid window. For calculating volume of the cells I used Measure_Stack.java Image J plugin from Bob Dougherty, the confocal image is first converted into 8-bit grey scale image, subtract the background noise and then measure volume of each cells.

2.10 Experimental Setup at (I-13)

Experiment was conducted at the coherence branch of beam line I13 at DLS which is renowned for generating wavelength range of hard x-rays along with cryo chamber developed by Prof Ian Robinson group's using synchrotron energy source and rabbit red blood cells samples was prepared at life science lab of **R**esearch **C**omplex at **H**arwell (RCaH).

Cryo-ptychography experiment setup consist of various important components through which beam passes and projected on the detector as diffraction patterns and at lastly reconstructed into images by ptychography i) Compound Refractive Lens (CRL) used for pre-focusing hard x-rays for better transmission of light by adjusting X and Y direction to find beam by adjusting pinhole position, increase scattering and the flux intensity on the sample plus reduce the signal to noise ratio ii) Undulator which makes coherent X-ray beam-collimated monochromatic X-light of energy 7.5KeV energy iii) 0.5mm x 0.5mm in size set by two pairs of slits used to create interference pattern of light: vacuum chamber v) 20um pinhole (I08 , DLS) placed; on which beam illuminates to form the probe wave on the sample placed 3 meter (m) downstream to sample vi) A Merlin detector with a pixel size of 55µm (Quantum Detectors, UK) was located 7.5 m downstream of the sample and used to acquire the diffraction patterns while the illumination pinhole was scanned vii) Inside the vacuum chamber; cryo chamber is attached with load lock shuttle (Leica, sample transfer equipment) and liquid nitrogen supply container continuously at interval of 60 minutes, attached to vacuum chamber opposite to each other (fig 2) and viii) Differential pumping of 8nm diameter,1.5mm thick and 1-6mm hole for pressure and turble pumping used to maintain the pressure, reduce air to avoid crystallization of water content occurring quickly and maintains vacuum environment inside the chamber. In this setup beam was fixed by using 20µm pinhole whereas sample was rotated and scan to get full field view image of the sample.

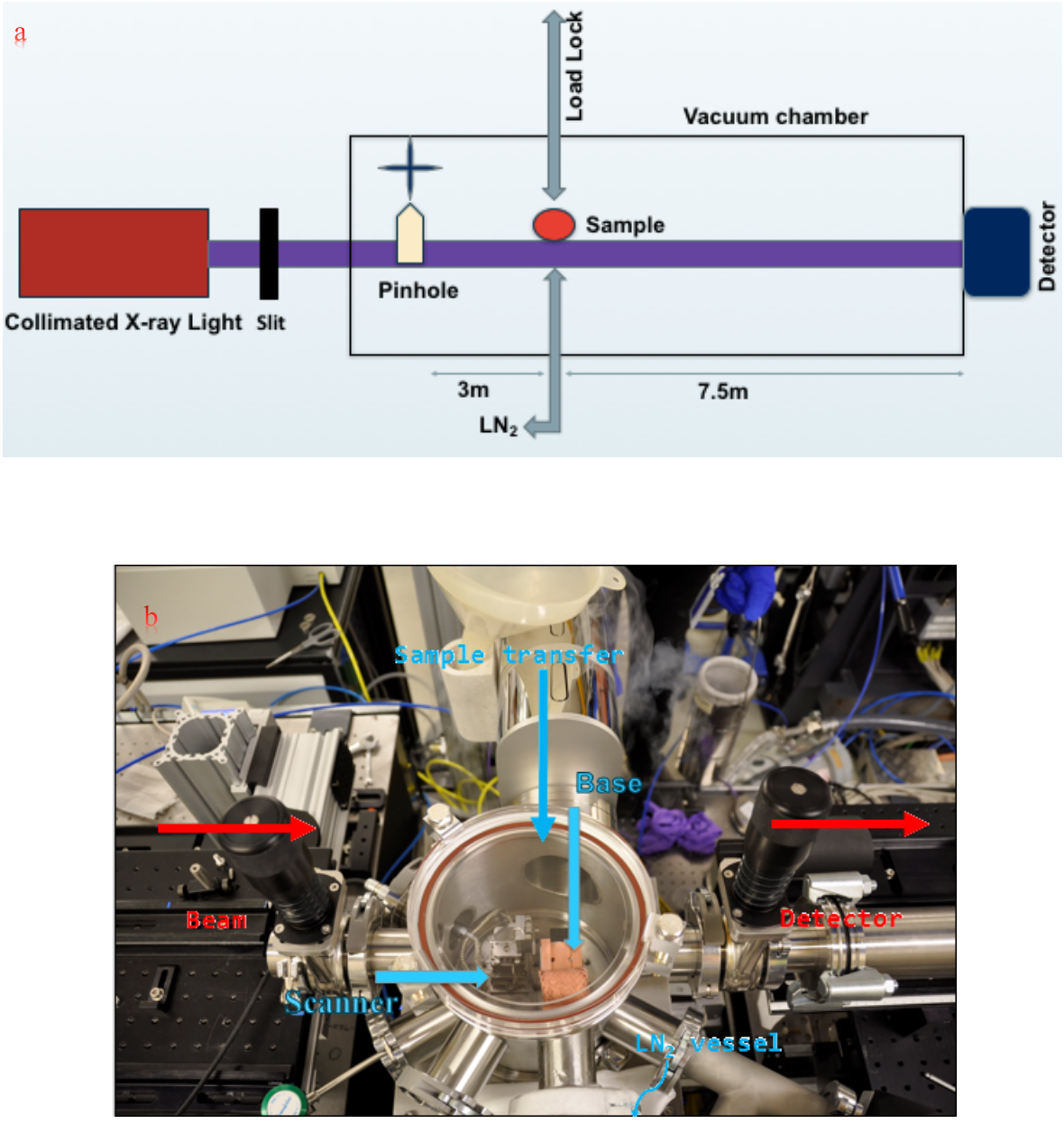

Figure 9 Experimental setup for cryo-ptychography experiment at I13 beam line of DLS, a) sketch diagram of vacuum sample chamber b) vacuum sample chamber.

The cold reservoir is made of a high current feedthrough attached to one of the vacuum flanges. It is connected to the sample holder by four layers of flexible copper stripes, attached with screws on both ends. The exterior end of the copper rod ends in a Styrofoam bath which was filled with liquid nitrogen in order to cool the sample holder. The liquid nitrogen evaporated over time, and the Styrofoam bath had to be refilled about once every 60min. The pressure inside the sample vacuum chamber was about 5 mbar during the measurements, without active pumping.

The samples were prepared by plunge freezing at RCaH and transported to the beamline in a liquid

nitrogen dewar, and then mounted on the copper plate inside a LN_2 bath. The sample was kept under LN_2 until the moment of the transfer into the vacuum chamber. For the transfer, the chamber was vented with argon to yield a dry gas environment and minimize ice formation on the sample. The top lid of the chamber was opened to the ambient environment and the copper plate with the sample was dropped into the receiver slot on the sample holder.

The ptychography measurements were carried out at 7.5 keV, optimizing the delivered flux and the focusing properties of the 400 μm **F**resnel **Z**one **P**late (FZP) to focus the beam, Spiral scanning is done to get 70% overlapping diffraction pattern to image and a MERLIN detector used for acquisition to obtain diffraction pattern for reconstruction into image.

3. RESULTS

Red blood cells are important components in organism which is responsible for transporting of useful nutrients to whole body and extracting out waste products from the body through process of osmosis. Aim was to study how osmosis occur in RBCs in different molar concentration of NaCL with addition of affect to the structure of the cells and ultimate effect due to structure modification to the body. To study these, I treated commercially available purified rabbit red blood cells in different NaCL salt concentration, adjusted its pH to obtained favourable condition such as isotonic, hypotonic and hypertonic to observe normal, hemolysis and crenation of cells respectively, validated the treated cells under confocal microscope by dropping cells on glass slides and TEM grids eventually validated sample with specific density was taken for x-ray imaging at I-13.

3.1 Cells treated in different solutions

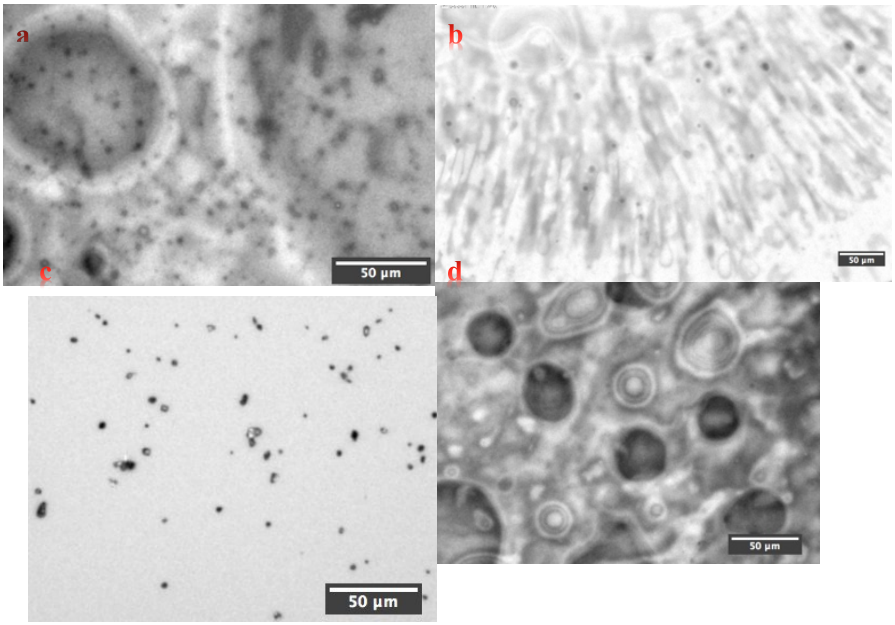

Figure 10 Grey scale snapshot of RBCs in different solutions observed under confocal microscope using 50x lens, cells indicated by arrows on each picture, scale bar-50µm a) commercially available pure RBCs in alsever solution b) 164mM NaCl c) pure distil water d) 1x PBS (10mM).

S.No	Solution	Diameter of cells (µm)	Volume of cells (μm^3)
A	**pure RBCs**	**3.37**	**30.51**
B	**164mM NaCl**	**2-7**	**65.65**
C	**Distil water**	**1.93**	**44.62**

D	**1x PBS**	**30.94**	**1089.87**

Table 3 Size and volume of different cells of Figure 1 calculated by Image J software.

Cells were observed on the glass under confocal microscope by 50x lens dissolve in different solutions to see the size and volume of the cells. 3µl of pure RBCs was dropped on glass slide (Supersoft) and covered with cover slip to observe under microscope before it gets dry, size ranges from 2-5 micron; cells in 164mM NaCl solution ranges from 2-7 microns, cells in pure distil water ranges from 1-2 micron that got completely disrupted and vanished and finally cells were treated in Phosphate Borate solution (1x PBS) size ranges from 13-31 micron, it swells and become ten times bigger than normal cells but does not burst. Diameter and volume of the cells were calculated using tools in Image J shown in the table.

3.2 Cells in different osmotic condition

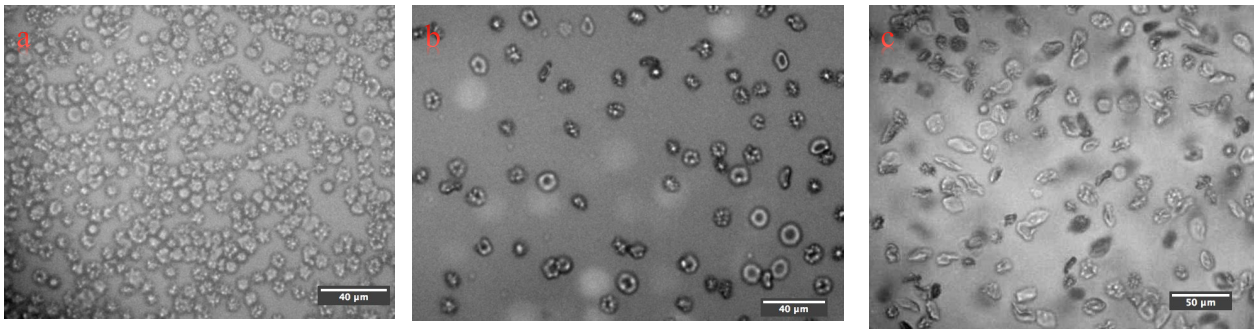

Figure 11 Grey scale snapshot from Image J software of RBCs treated with different NaCl concentration observed under 50x lens of confocal microscope a) Isotonic condition of 164mM NaCl, scale bar 40µm b) Hypotonic condition of 103mM NaCl, scale bar 40µm c) Hypertonic condition of 1.7M NaCl, scale bar 50µm.

S.No	Osmolarity concentration	Diameter of cell (µm)	Volume of cell (μm^3)
A	**Isotonic (164mM NaCl)**	**5.3**	**73.13**
B	**Hypotonic (103mM NaCl)**	**12.25**	**215.74**

C	**Hypertonic (1.7M NaCl)**	**14.96**	**262.60**

Table 4 Size and volume of the cells calculated using Image J tools in Isotonic, Hypotonic and Hypertonic concentration of NaCl.

Cells in Isotonic, Hypotonic and Hypertonic salt concentrations were dropped on glass slide were observed under confocal microscope by 50x , cell in 164mM NaCl remain normal size of 3-6µm plus with good density of cells on the slide, Hypotonic concentration shows swollen of size 8-14µm; distorted structured and shrunk cells size 2-4µm and with less density on the slide compared to the Isotonic finally Hypertonic concentration shows crenated cells which means water content from the cell lost due to osmosis and cells become elongated and shrunk of size 9-15µm addition to that less density as cells start dying.

3.3 Chronological order salt concentration

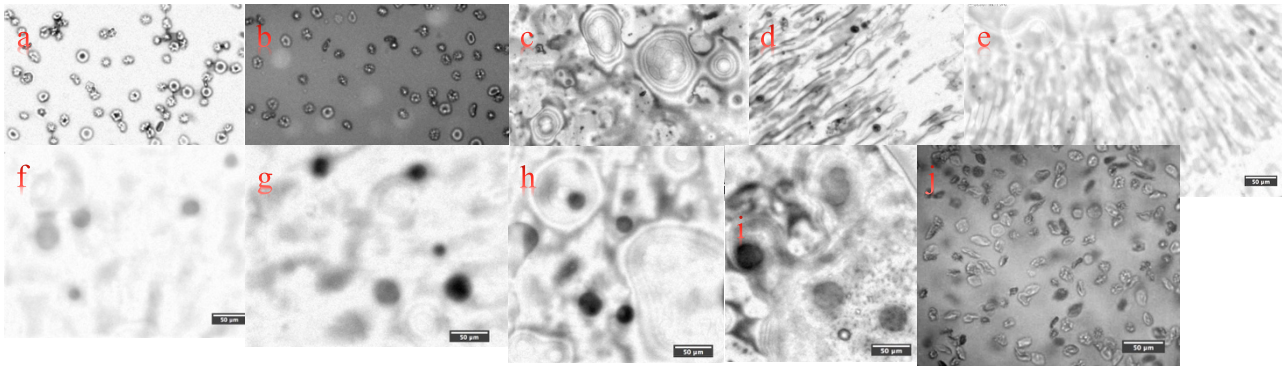

Figure 12 Grey scale snapshot from image J of RBCs which is serial diluted in NaCl salt ranges from a-b with scale bar of 40µm (89mM and 103mM), c-j with scale bar of 50µm (123mM, 144mM, 164mM, 185mM, 205mM, 226mM, 246mM and 1.7M) taken from confocal microscope.

Concentration (mM)	Length (µm)	Circularity	Round	Volume(µm3)
89	12.91	0.999	0.904	220.696
103	12.252	0.783	0.892	79.257
123	16.619	0.954	0.646	199.656
144	9.34	0.992	0.931	232.78
164	3.164	0.993	0.81	65.653
185	15.069	1	0.919	391.101
205	26.115	0.98	0.799	235.773
226	22.296	1	0.971	447.025

246	34.626	1	0.98	1113.604
1711	14.959	0.777	0.813	262.593

Table 4 This table represents the diameter, circularity, roundness and volume of the rabbit RBCs treated in different concentration of NaCl salt.

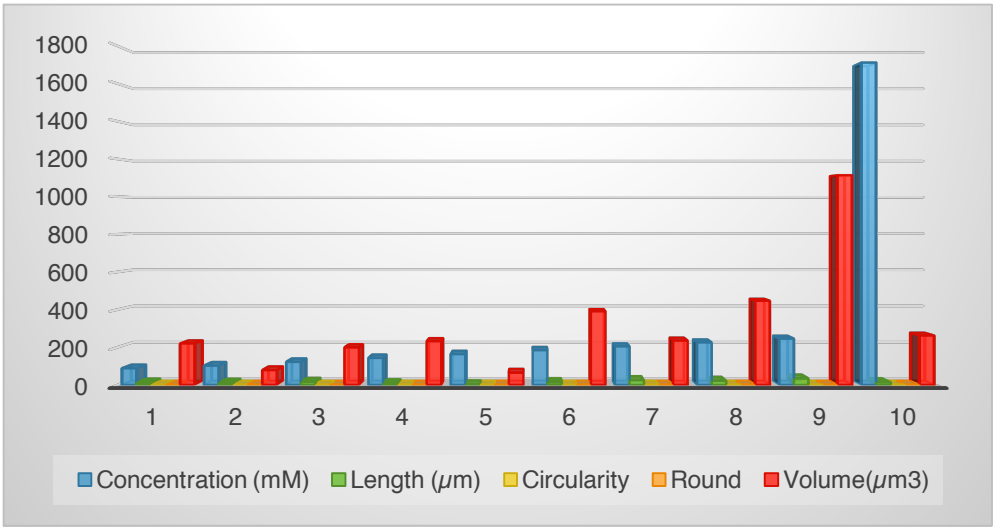

Graph 1 3-D clustered column graph represents effect of NaCl concentration on the length, circularity, round and volume of the cells with increasing NaCl concentrations. Column starts from concentration (blue), length (green), circularity(yellow), round (orange) and red bar represents the volume of the cells as shown on the graph.

This experiment was done to see the gradual change in the diameter and volume of the cells due to change in NaCL salt concentration but we could see the significant change in the cells from 86mM to 1.7M dilutions. Red blood cells were prepared in NaCl solution, spun down at 1000 rpm for 10mins in centrifuge and later taken for observation under confocal microscope. From figure (a, b, j) it is predicted that cells are in extreme condition of hemolysis and crenation because of that it showed wide variety of cell size and volume whereas from figure (c-i) shows increasing size of volume and size of the cells as concentration of NaCl is increases chronologically. The circularity of cell increase with increasing concentration except with 103mM NaCl- it has more varieties of cell whereas round shape of the cells differs randomly in each concentration as shown in the table 2.

3.4 Sample Grids before X-ray beam hits

Rabbit Red Blood Cells sample prepared in Isotonic (164mM), Hypotonic (103mM) and Hypertonic (1.7M) salt concentration, spun down in centrifuge at 1000rpm for 10mins, fixed with 2.5% glutaraldehyde chemical fixative; dropped 5µl of sample onto the hydrophilic silicon nitride window grids which was treated with poly-L-sine before use and washed with distil water 2-3 times in order

to remove salt deposition from the grids and then placed on the 3mm sample carefully with tweezer for x-ray imaging. Grids were imaged before and after the hits furthermore to notice radiation damage to the sample and the grids.

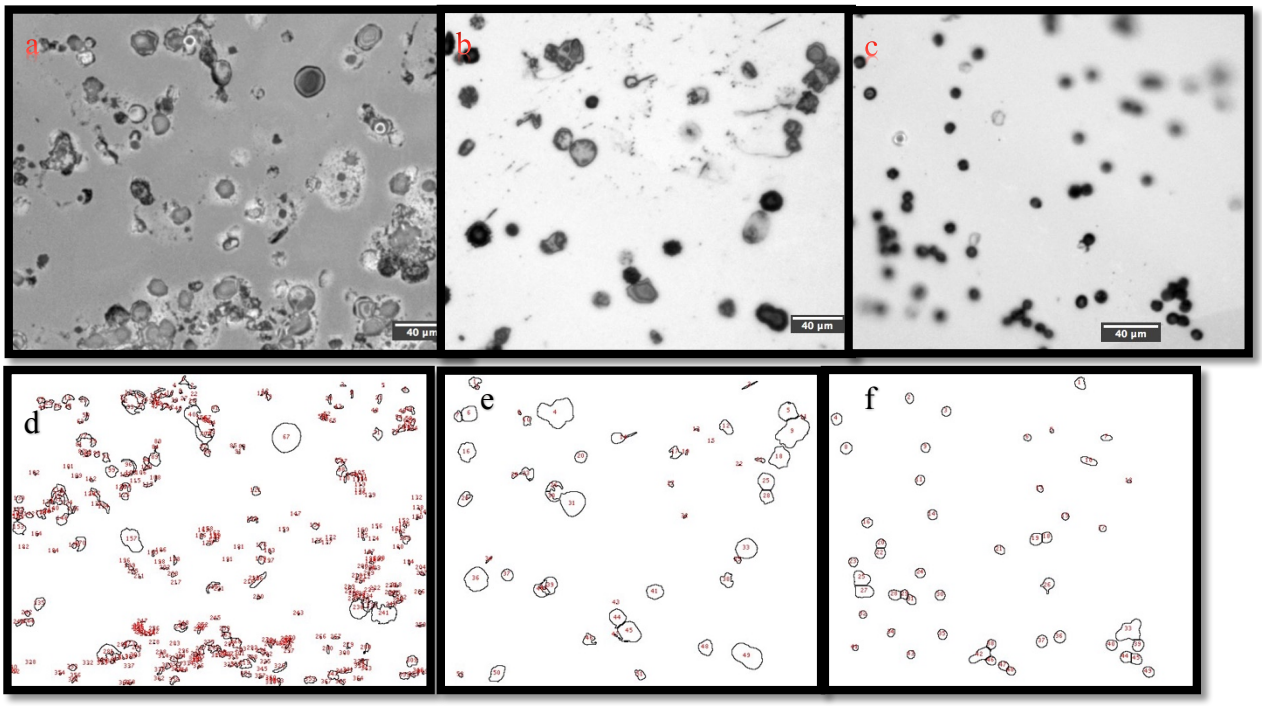

Figure 13 Grey scale snapshot of a) Isotonic (normal cells), b) Hypotonic (swollen and burst cells) and c) Hypertonic (shrunk and elongated cells) RBCs sample and the cells present on silicon nitride window, scale bar is 40µm. Image d-f are cell counts of Isotonic, Hypotonic and Hypertonic respectively calculated from Image J.

Silicon nitride window imaged whilst inside sample holder by confocal microscope, Images show the cells plus deposition of salt concentration, which we try to reduce by washing it with distil water. Number of cells counted by Image J in a particular selected area of silicon nitride window- Isotonic has 370 cells, Hypotonic has 52 cells, and Hypertonic has 49 cells.

3.5 Sample grids after x-rays beam hits

Sample grids were imaged whilst inside sample holder after they finished several scan on different area of silicon nitride at different field of view to target maximum number of cells for imaging at room temperature under confocal microscope. Images were processed in Image J in order to calculate the number of cells presents after scan and also to observe radiation damage to the cells and the grids which will help to measure the number of radiation dose to our biological sample. Imaged processed with Image J reduces the background contamination like salt deposition and analyze particle tools

only count red blood cells and distinguish from salt concentration. Image J exclude the cells present on the edge of image and gives exact number of cells while processing with wheatshead tool.

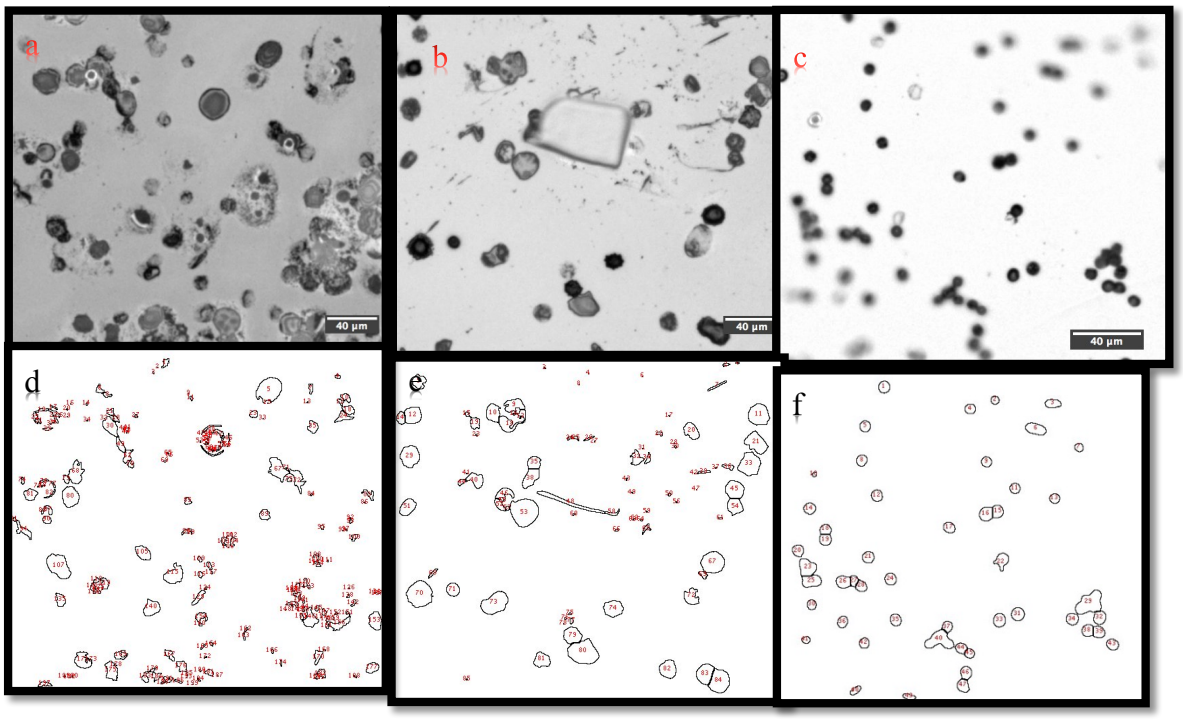

Figure 14 grey scale image of x-ray scanned sample on Si_3N_4 grids of cells, scale bar-40µm a) Isotonic cells can be seen with more salt deposition b) Hypotonic grid with swollen cells as well as bursting stage of the cells and the broken piece of Si_3N_4 plus with less salt deposition c) Hypertonic grids shown shrunken cells and also very less deposition of salt compared to other two grids. Image d-f are cell counting on specified area of each grids from Image J.

Cell counting after x-ray scan show bit different counting compared to before x-rays hits such as Isotonic has 199, Hypotonic has 85 and Hypertonic has 49 this could be because of imperfection adjustment of threshold- which also count background signals and gives unexpected counting or may be little difference in area selection while image processing. The broken piece of Si_3N_4 window is not visible on the processed image (e).

3.6 Cells onto different TEM grids

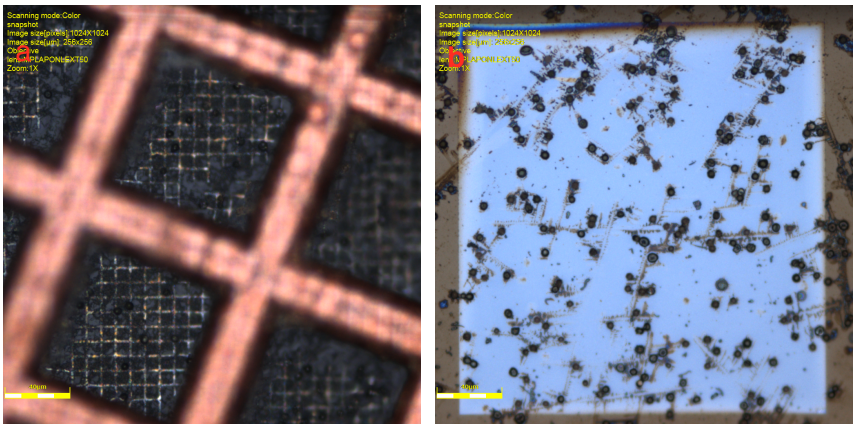

Figure 15 a) 7 x 7 μm^2 holes carbon film with thick carbon bars but it looks thin carbon films are damaged and b) 250 x 250μm^2 silicon nitride window TEM grids is in good condition. Imaged taken under confocal microscope using 50x lens, scale bar-40µm.

Both grids flooded with 1.25% glutaraldehyde fixed RBCs to see the density of cells onto grids and capacity of grids to withstand fixed cells under room temperature. It was observed that 7 x 7 μm^2 bars of thin carbon film started breaking slowly as sample was drying but thick bars were stable on the other hand Si_3N_4 membrane did withstand 1.25% glutaraldehyde fixed sample and good density of the sample can be seen on the grids after drying. Small circular black spots on the grids are density of RBCs plus salt deposition was also observed on the grids which has possible to give more background signal.

3.7 Experiment under liquid nitrogen

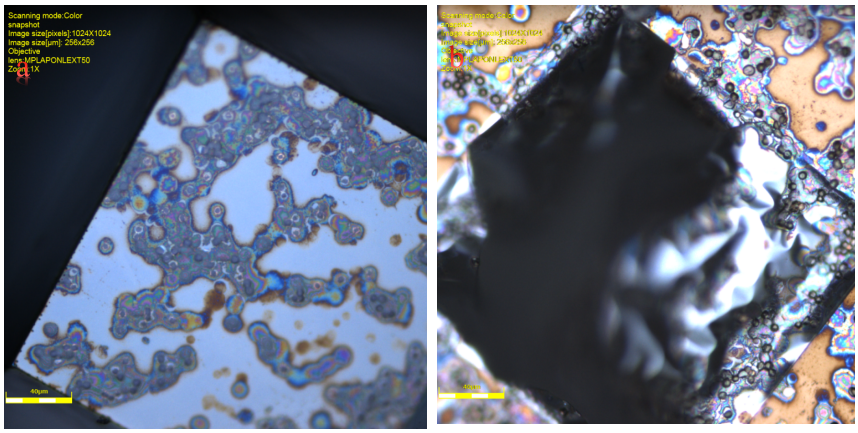

Figure 16 Confocal microscope image of Si_3N_4 membrane flooded with 5µl of heavly dense 164mM NaCl, glutaraldehyde fixed RBCs in sample holder, scale bar-40µm. a) Image of grid before x-ray hits shows circular red blood cells visible along with excess deposition of NaCl salts on membrane b) Spread of red blood cells and traces of NaCl salts deposition observed under microscope after x-rays hits plus it was also observed that

membrane was completely shattered. RBCs sample was prepared at room temperature then kept into cryo vacuum chamber in liquid nitrogen environment in I13 beamline while imaging to see ice formation on the grid. Sample was to dense so they were blotted 2-3 times to reduce the concentration of salt from the grid and get clear RBCs but cells was completely mixed with salts and clumped together was bit difficult to distinguish to both them. It was observed that Si_3N_4 window was completely shattered after the beam hits and very less sample was left, this could be because of thermal pressure, mis-handling while placing inside the chamber or due to beam hits.

3.8 Ptychography Reconstructions of Nuclei

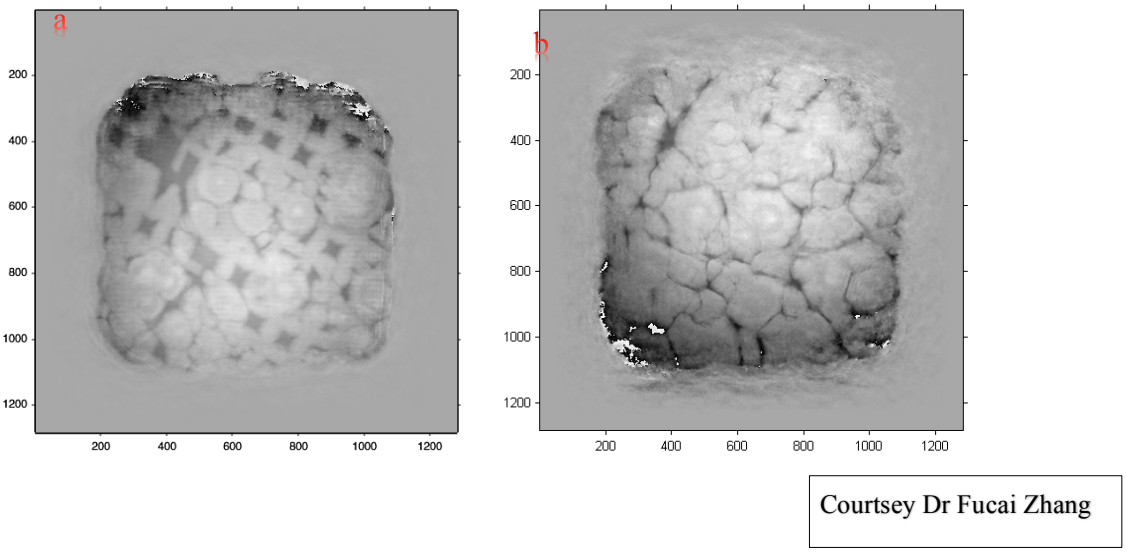

Figure 17 Phase reconstructions of 7 x 7 μm^2 carbon quantifoil representing the cell nuclei and ice scattered on the carbon grids and at field of view (FOV) of 30µm x 30µm. a) reconstruction of image at scan 3 of quantifoil b) reconstruction of image at scan 8 of quantifoil.

Quantifoil was covered with some nuclei of the cells and mostly spread with ice and as the number of scan preceded, ice build can be seen very clearly and eventually whole quantifoil is covered with ice formation from scan 3 to scan 8 and was difficult to find traces of chromosomes with which grids was flooded with but unfortunately we can see the traces of cell nuclei but not the chromosome furthermore it shows that ice formation was very quick due liquid nitrogen present inside the cryo vacuum chamber. It is also visible that bars of carbon film also got broken probably by scan, during sample preparation or from thermal pressure.

3.9 Diffraction Pattern

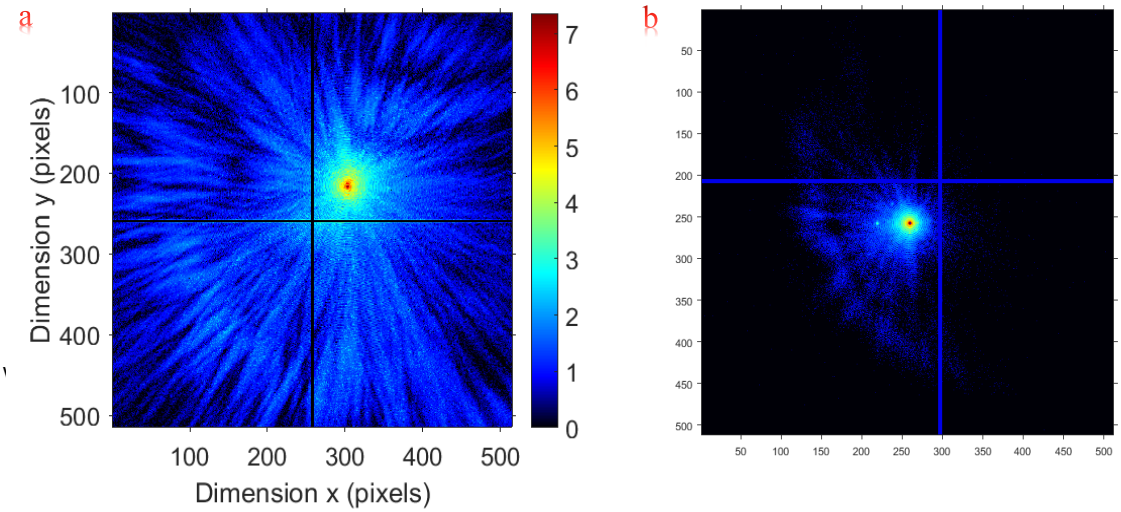

Figure 18 a) one of logarithmic scale diffraction pattern obtained from plunge frozen chromosome sample in a liquid nitrogen condition b) log scale diffraction pattern obtained from one of glutaraldehyde fixed rabbit red blood cells sample at room temperature.

On chromosome prepared sample; logarithmic diffraction signals spread widely to the edge of the detector of 55µm merlin detector. The highest diffraction signals widely to the edge of the detector. The highest diffraction angle determines the image reconstruction resolution, which was about 160nm for our experiments. In red blood cells logarithmic diffraction are more spread close to the center rather than spread over all detector plus diffraction pattern are not very bright unlike chromosome diffraction pattern. Bright sides show more photon counts and dark side shows less photon counts. High intensity diffraction pattern shows that object is very complicated so it needs computer algorthim to reconstruct into images because manipulated manual is not possible, logarithmic scale is plotted because it enables to see both weak and high contrast both on the images. The circular ring shows that object is sphere. Speckle pattern is used to determine the sharpness and roughness of sample

4. MOTIVE OF THE EXPERIMENT

The aim of the experiment was for testing a new cryogenic sample environment for use in ptychography at I-13 DLS, in particular for imaging of biological samples. The goal was to prepare biological samples with the plunge freezing method, and transfer the sample into the beam line vacuum chamber without crystallization of the water content. The biological samples are then imaged using the x-ray ptychography method, which requires numerical reconstruction of a set of diffraction patterns. Biological samples investigated are structure of human chromosomes and nuclei on the 20 nm scale resolution, rabbit RBCs treated with NaCl salt fixed with glutaraldehyde chemical and eventually horse spleen ferritin protein crystal which is due in September 2016.

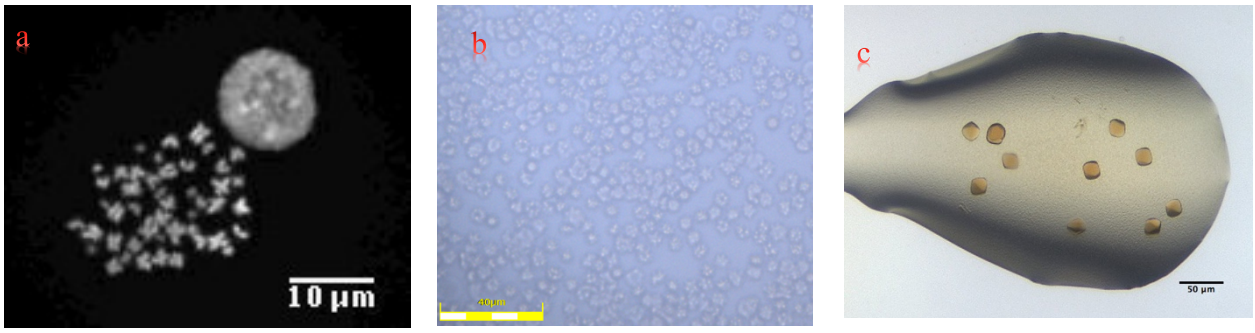

Figure 19 Different biological sample investigated in novel cryo chamber a) MAA fixed human chromosomes and nuclei image taken from fluorescence microscope, scale bar-10µm b) rabbit red blood cells in NaCl saline solution imaged by 50x lens of confocal microscope, scale bar- 40µm c) Horse spleen ferritin crystallized using robotic system at oppf at research complex, scale bar-50µm.

Methanol **A**cetic **A**cid (MAA) fixed and 4,6-Diamidino-2-phenylindole (DAPI) stain human chromosomes with nuclei were plunge frozen observed under fluorescence microscope (Zesis) for validation. Some sample were stained with platinum blue at room temperature for better contrast image and some were vitrified samples in their native state. The main objective of this beamtime was to attempt a cold transfer of a cryogenically frozen sample into the LN_2 environment, and to perform ptychographic imaging of chromosomes; important parameters were, distance between sample and detector was15m, incident energy was 7.5KeV and plunge frozen sample on TEM grids, fortunately we able to do few ptychography scan and obtain some ice covered sample grids that made bit difficult to obtain native state chromosomes and other drawback was lost & damaged sample while transferring. Obtained result encouraged us to improve our cryo system to reduce the speed of ice formation on the sample.

Our next sample was rabbit red blood cells which has almost same size as chromosomes for imaging using same setup but with reduced ice formation by changing certain parameters such as distance between sample and detector which was 7.5m, incident energy of 7.3KeV, spatial resolution of <100nm, using CRL for focused beam and differential pumping of 0.1mbar in order to maintain the pressure and avoid crystallization in a vacuum chamber. Number of different osmotic RBCs sample were plunge frozen but unfortunately could not use it for experiment because Leica sample transfer system was broken which let us do chemical fixation using glutaraldehyde and image dry sample using ptychography x-ray scan at room temperature. In addition, we try to image at least one sample in LN_2 environment but sample prepared by chemical fixation at room temperature to measure speed of ice formation on the sample grids and reconstruction of ptychography x-ray scan is in process. Parameters for this scan were intensity of beam was 0.787×10^{-6}A, 250 x 250 μm^2 Si_3N_4 membrane and spiral scan to cover most of area of the window. With good practice with handling sample in liquid nitrogen let us rethink to propose another biological sample for imaging and work on icing reduction.

Future sample is imaging vitrified horse spleen ferritin crystal. Size of crystals (fig 18c) is approximate 20μm obtained using vapour diffusion method but novelity of our experiment is to measure small crystal cluster of ferritin that is around 1-2 micron in size on which still needs to be work on using same cryo-ptychography method to obtain crystal diffraction pattern for reconstruction by ptychography iterations and try to reduce the radiation damage plus icing on the sample grids.

5. DISCUSSIONS

In this report I try to reveal the size, shape and volume of the rabbit red blood cells which were treated under osmotic conditions (Isotonic, Hypotonic and Hypertonic) in NaCl salt concentrations and fixed in glutaraldehyde, imaged in a vacuum chamber at I 13 diamond using synchrotron hard x-rays energy, good quantitative diffraction patterns were obtained and further reconstructed using ptychography technique to obtain phase contrast image of RBCs. This experiment was followed up experiment of imaging of **M**ethanol **A**cetic **A**cid (MAA) fixed metaphase human chromosomes and nuclei. Main motive of these experiments was to reveal structure and morphology of biological samples in their native state using unique correlation of cryo-ptychography technique. RBCs samples were prepared in different molar NaCl concentration without and with glutaraldehyde fixative in parallel were observed under confocal microscope for validations. Normal shape, hemolytic and crenated morphology of RBCs can be easily seen by 50x lens of confocal microscope using lext software. Diameter, volume and counting of cells under certain field of view (FOV) were calculated using Image J software.

5.1 Hydrophilization of Grids

Two different grids i) silicon nitride (250 x 250 μm^2 window size) with thickness of 30nm and ii) carbon- coated quantifoil grids (7 x7 μm^2 square holes) were selected for spreading red blood cells on top. It was important to make the surface of the grids hydrophilic as the NaCl salt solution in which RBCs were prepared would not settle on the hydrophobic surface. Successful methods used were poly-L-sine solution for 30min treatment and glow discharge; grids treated with both the methods did showed some noticeable changes such that it was observed that quantifoil were not hydrophilic, though Si_3N_4 window were hydrophilic but for shorter time in a poly –L-sine solution whereas with glow discharge both the grids were hydrophilic and the samples evenly spread can be easily be seen under confocal microscope. But the negative part of these methods was that hydrophilic nature of the carbon film would last for 20-30mins whereas for the Si_3N_4 window would last for the 50-60 mins after this they were not usable anymore.

5.2 Resistance of Grids

Sample presence on grids was examined by dropping it on the grids which was then observed under a confocal microscope before x-rays imaging. It was noticed that inner grid bar of qunatifoil was getting dissolved slowly due to gultaraldehyde chemically fixed sample drying at room temperature or due to heat from the confocal microscope lens. This made difficult to see the sample on the grids, but the larger bars of quantifoil still survived. Recovered quantifoil from the beam line also had broken grids which might prove that quantifoil was not good quality that could not resist the either glutaraldehyde chemical or was not of good heat resistance.

Silicon nitride window looked undamaged while scanning under confocal microscope; it could resist the glutaraldehyde -fixative at room temperature. When the sample was recovered after x-ray experiment, the silicon membrane was broken that might be due to mishandling while transferring into holder or taking it out at room temperature after several scans.

5.3 Method to reduce the salt concentration from the grids

Sample was centrifuged at 1000rpm for 10min in order to reduce the deposition of salt on the grids because centrifuge let the salt settle down and sample on the top in the solution, for examination supernatant was used rather than pellet to suppress the salt deposition and avoid hinderance while scanning to obtain valuable diffraction pattern of RBCs. Second method was to wash with distil water 2-3 times and then wiped excess amount of liquid using filter paper to decrease the concentration of salt after dropping the sample on grids, though it was difficult to wipe as there was chance to loose sample from grid and also grid fly off while handling and was critical aspect of sample preparation for the x-ray imaging furthermore we manage to follow both the methods for better results. Some other issues while loading sample on the grid was adding excess sample that lead to damage of membrane and bar of grids or could be mechanical stress while loading and blotting samples.

5.4 Peculiar shapes of RBCs

Image J software tool used to measure the shape, size and volume of rabbit RBCs treated under different molar concentration of NaCl starting from 89mM to 1.7M in a chronological order in order to measure the gradual change in shape of RBCs

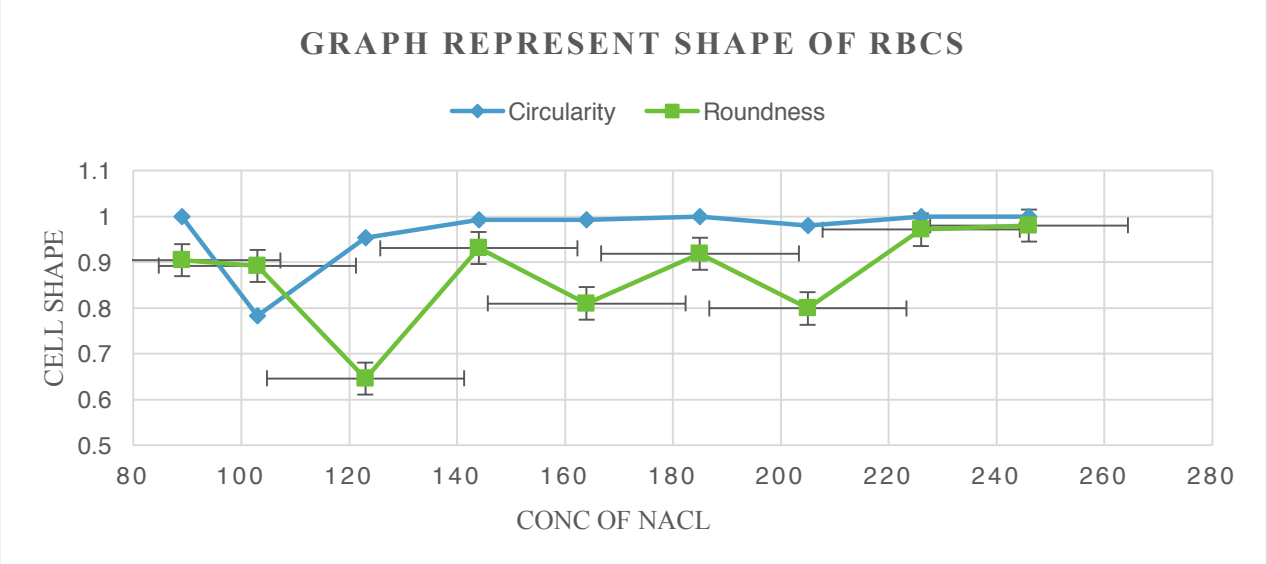

Graph 2 Line graph with marker shows difference between circularity and round configuration of RBCs in a chronological order starting from hypotonic solution (89mM) to hypertonic solutions (1.7M) of NaCl concentration (x-axis). Error show the graphical difference and error.

The main difference between circle and round is that circle is 2 dimensional flat surface with constant radius whereas round is 3 dimensional with varying radius, this could be the reason that its shows huge fluctuation in cell configuration. Line graph with marker shows that circular configuration of RBCs has less variation compared to round configuration of the RBCs at preceding order of sample prepared in NaCl concentrations from hypotonic to hypertonic solution. As we know that one is perfect circle and above graph 2 represent that 103mM-hypotonic solution is less circular than other molar concentrations and it became circular again at normal at 144mM-185mM concentration NaCl and sustains it healthy biconcave disc shape. Furthermore, more it changes its configuration as it reaches to hypertonic concentration.

5.5 Diameter, Volume of Rabbit Red Blood Cells

Species	Diameter (um)	Volume(um^3)	Life Span
Human	7.3	95	120 days
Rabbit	6.1	76	57 (6)
Pig	5.81	61	-
Mouse	5.8	41	-
Rabbit (experimental value)	5.3	73.13	57

Table 4 Literature and experimental value -diameter and volume of rabbit red blood cells in microns calculated by image J.

As mentioned above under introduction section that rabbit RBCs is morphologically similar to human RBCs and table 4 supports the statement. Experimentally obtained diameter of rabbit RBCs ranges from 2-7 microns (table 2). There are millions of RBCs in rabbit and they all with varying shape and size this could be the reason that average value calculated experimentally is bit different from literature or might be the experimental and calculation error.

5.6 PBS Treated Blood Cells

Cells treated with 1x PBS were just swollen and were approx. 10x bigger than normal cells but still they don't burst whereas in hypotonic condition cell swells up and finally burst and in hypertonic condition it loses its water content and become crenation. In isotonic the solvent and solute concentration remains constant, hypotonic the water as solvent enters into the cells and makes it

swollen and finally burst followed by dying or vanished eventually Hypertonic concentration waters squeeze out from the cells and it loose its biconcave structure and becomes elongated.

5.7 Radiation Damage to Biological Samples

Radiation damage is one of the limiting factor for the x-ray imaging of biological samples. Aim of the experiment was to see the radiation damage to the RBCs went through x-ray hit, but unfortunately we could not see significant radiation prints on the sample and on the grids with confocal microscope as depth of lens is not enough to measure the radiation spot plus internal structure of the cells. We assume radiation would affect the radiosensitive spectrin monomer- which tangled to form membrane for the RBCs and breaks connective fiberes of spectrin according in addition, morphology of the samples also remains similar to before and after beam hits.

Biological sample are more prone to radiation damage because it contains 70% water molecules so as RBCs, Therefore, Biological sample needs to be imaged in hydrated state close to native state. To keep sample hydrated it needs to be plunge frozen to reduce the radiation damage caused by x-ray exposure. Chemical fixation maintains the integrity of the internal structure and volume of the cells but it destroys the external structure of the RBCs to some extent which will be hinderance to understand the morphology and cellular function of the cells which is difficult to measure by normal optical and confocal microscope. As we can see from

Radiation depend upon flux density, temperature, concentration of salts, hydration, chemical and incident beam characteristic (55) and radiation is strong enough to change the chemical and physical characteristic of cells. As we could not see any radiation damage except broken piece of Si_3N_4 (fig 14) that made me assume that glutaraldehyde fixed sample flooded on grids protects the cells from mechanical stress, atmospheric pressure and radiation damage which is not noticeable my confocal microscope until it's been reconstructed using numerical technique of ptychography. It was observed that glutaraldehyde fixed samples still maintains its structure without much distortion even after dehydration whereas sample in LN_2 (fig 15) after beam hits shows some radiations damage that could be the reason for its window breakage or it would have broken during mishandling. Second reason could be that the intensity of the beam of not intense or fixed enough to measure radiation tolerance on the sample grids and it was fluctuating.

5.8 Morphology of Red Blood Cells

As we know that RBCs exits in different shapes and size in plasma of organisms. From my results section (fig 11a) it proves the statement as image is taken in their native state in isotonic NaCl solution observed under confocal microscope without any fixation. RBCs imaged without glutaraldehyde

fixation has varied features and characteristics in different osmotic pressures (Isotonic, Hypotonic, Hypertonic), every cells has special appearance, spikes, size, circularity, roundness and shape from figure 10 whereas cells which are glutaraldehyde fixed has almost similar shape and no spikes at the membrane of the cells which can be easily be compare from figure 11c to figure 13c & 14c, the cells are more round and smooth without much spikes noticeable no matter what is the salt concentration. This proves that glutaraldehyde chemical does affect the morphology of the biological samples (RBCs) and squeeze the cell towards inward of the cell by releasing some water content of the biological samples eventually it proves that chemical fixation is not good method for imaging biological sample to its native state. Significant loss of volume, chemical conformation and morphology of the cells by chemical fixation.

5.9 Rate of Ice Formation

Calculating the speed of ice buildup and thickness of ice on the sample grid is a challenging task. Main challenge is the transfer of cold sample into the vacuum chamber on the beamline while preventing ice formation. During the transfer into the chamber ice formation was visible on the copper feedthrough, and on the copper plate that the sample is attached to. The copper block sample holder showed some condensation and probably ice formation but because of using pump most of the ice were evaporated.

The most temperamental parts of the sample preparation are plunge freezing were transferring vitrified sample grids from liquid ethane to cryo holder kept in LN_2 that has possibility of ice formation if it's been not done instantly with precautions and second one is procedure of transferring the sample grid under liquid nitrogen to the sample holder as these two process involved keeping all components (tweezers, the screw opener, cryo holder) cool in liquid nitrogen. There is the severe risk of ice crystal formation if any mistakes were made. Enough liquid nitrogen should be there in foam dewar to get drowned all components plus able to see through it to operate sample transfer.

For my next experiment at I13 beamline with ferritin protein crystal I am using cryo-protectant glycerol while sample preparation to minimize the ice formation on the sample grid that will reduce the formation of ice while sample transferring from cryo-station to cryo-chamber in liquid nitrogen environment and ultimately it will protect my sample from thermal stress in parallel it will avoid breakage of TEM grids.

5.10 Red Blood Cells in extreme saline condition

RBCs are biconcave disc shape structure containing hemoglobin protein which is quatnary structure. Phospholipid bilayer membrane of RBCs which maintains the inflow and outflow of water and other ions & solute in addition develop osmotic pressure plus it also maintains the internal structure of cells from unwanted solute and mechanical pressure. In hypotonic condition the solute concentration is

more inside the cells that lead cells to swell up, burst and vanished that's why we see less amount of RBCs. In hypertonic condition its other way round the solute concentration is more outside the RBCs which leads to shrinkage & crenation of cells, it looks that it take more time to vanish cells compared to hypotonic osmotic pressure as it has more cells shown in fig 11c. It is concluded from the results that cells should always be in isotonic condition and maintains it solute and Na^+, K^+ and Cl^- in the RBCs plus cytosol by which its surrounded (27). Cells die in extreme condition before its actual life span which is 120days in human, it only last for 40-50days eventually leads to renal chronic anemia disease (61) which even carry to further serious situation as the block the blood vessels. Blood pressure is also an issue due to imbalance intake of NaCl concentration, especially due to Cl^- ion (Theodore, 2005). it maintains the internal structure of RBCs plus regulates the movement of solvent, lipid bilayer membrane of RBCs sustains the morphology and make it stiff to withstand osmotic pressure in addition, protects from various disease occurring because of membrane lose such as hereditary elliptocytosis, spherocytosis etc (62). In uremia when kidney fails to excrete out nitrogenous waste and accumulate urea in blood this leads to osmotic pressure and cells shrinks & crenate eventually reduced in number (61). Its seems that we need equal amount of NaCl salt in our body to maintain volume of cells and enable continue flow rate of RBCs through blood vessels.

5.11 Issue with ptychography reconstruction

Ptychography iterate between real and reciprocal space, it provides good structure information with high resolution but limited with providing chemical composition of the samples. Samples were imaged using x-ray ptychography scan. Several scans carried out for ptychography reconstructions were attempted but so were not successful. It is more difficult than usual to retrieve a good reconstruction of the test sample and the illumination function. The reason for this might be related to the unknown phase curvature in the sample plane. We are continuing to work on the reconstruction of this data, as we believe that a better modelling of the illumination function will result in successful phase retrieval.

6. FUTURE PLANNING

6.1 Short Term Goal

Aim in my next experiment from 7th – 13th September 2016 is to reduce the ice formation on the sample grids plus in the cryo-chamber by doing some successful plunge freezing ferritin crystals and to measure the radiation dose on the sample and try to resolve the radiation damage to the biological sample which is peak research for many scientists working with X-rays by analyzing imaged reconstructed by ptychography phase retrieval method which has power for high resolution reconstructions. In addition, I will also validate my plunge frozen sample in a cryo TEM to see thickness of ice formation on the samples before taking them for x-ray imaging at I 13 beam line. This act would help me to compare results of plunge frozen ferritin crystal at their native state with glutaraldehyde fixed RBCs to calculate ice formation and radiation damage of biological samples used in novel cryo-ptychography chamber developed by Prof Robinson's group. And my second aim is to write a proposal to do experiment at ID16 beamline; **E**uropean **S**ynchrotron **R**adiation **F**acility (ESRF) Grenoble, France to do cryo experiment with plunge frozen human chromosomes samples prepared in RCaH, Oxford, using new build LEICA cryo sample transfer system which will be held in between March and July 2017 if accepted, this will also be good opportunity to measure thickness of ice buildup while sample transferring from obtained results. Third to find out why red bloods cell in 1x PBS does not burst even though their size increase 10x more than the hypotonic solution.

6.2Long Term Goal

Goal is to study the radiation damage to the human chromosomes and study repair mechanism after the radiation damage using **F**luorescence-**L**ifetime **I**maging **M**icroscopy (FLIM) under supervision of Dr Stan Botchway and Dr Mohammed Yusuf which is continuation of PhD thesis of Ana Estandarte- student of Prof Robinson. Second is to analysis 40 000 diffraction pattern data of human chromosomes obtained by Prof Robinson's group using **X**-ray **F**ree **E**lectron **L**aser (XFEL) facility from SPring-8 Angstrom Compact Free Electron Laser (SCALA), Japan. To analysis this I got offer from Prof Nishino Yoshinori, Hokkaido Japan to learn some image analysis techniques in his laboratory.

7. CONCLUSION

The main objective of these experiment is to image biological sample (human Chromosomes, rabbit red blood cells and horse spleen ferritin protein crystal) in their native state using cryo chamber develop by Prof Robinson's group. The main objective was to attempt a cold transfer of a cryogenically frozen sample into the LN_2 environment, and to perform phase retrieval ptychographic x-ray scan for imaging of biological samples and from these reconstructions calculate the rate of icing and radiation damage to the samples.

Rabbit red blood cells were treated with different concentration of NaCl salt in order to measure the degree of morphology changes of cells in extreme conditions (Hypotonic and Hypertonic) of salt in organism and I observed that morphology of the RBCs changes with change in concentration of NaCl buffer observed under confocal microscope; so, it's important that cells are maintained in Isotonic solution to avoid swelling, hemolysis and crenation of cells and have appropriate amount of salt intake in our daily dietary. From my experiment I conclude that osmosis is important process of an organisms to transport of oxygen, nutrients, and excrete out waste products from the body through various organs eventually maintains the morphology of RBCs, this process also avoid various disease caused due to extreme alterations such as anemia, block blood vesicle, chronic renal failure and probably cancer due to development of unwanted vesiculation mentioned in nature news; these disease occur due to change in structure and morphology of RBCs. Constant blood flow maintains blood pressure, temperature, pH and osmolarity of ions & minerals in the body and damage of it blocks the vessels and eventually stops the functioning of metabolism.

Study of RBCs morphology by X-ray in a cryo- close to native state, would give better picture to molecular to atomic level information which will be helpful to understand various disease caused by change in the shape of RBCs and from there genetic information can be fetch that leads to dangerous RBCs diseases, furthermore, it will be carried to hospitals for disease diagnosis and screening such as cell count in anemia patients.

Working on cryo transferring system to transfer samples in cold surrounding to avoid icing is a very time consuming and critical part for the sample preparation process plus maintaining constant flow of LN_2 is also tiring process while imaging. We did conduct a number of ptychography scans for reconstructions but unfortunately due to limitation of time I don't have enough results to conclude icing and radiation damage of the RBCs and we are still working on the ptychography -phaser retrieval algorithms.

8. REFERENCES

1. Johann Schaller, Simon Gerber, URs Kampfer SL and CT. Human Blood Plasma Proteina: Structure and Function. 2008.

2. Zhang Z, Cheng J, Xu F, Chen Y, Du J, Yuan M, et al. Red Blood Cell Extrudes Nucleus and Mitochondria Against Oxidative Stress. 2011;63(July):560–5.

3. Manuscript A. NIH Public Access. 2010;35(5):382–8.

4. Rob Phillips, Jane Kondev, Julie Theriot, Hernan Garcia NO. Physical Biology of the cell. Second. 2013.

5. Berg, Jeremy M, Tymoczko JL SL. Hemoglobin Transports Oxygen Efficiency by Binding Oxygen Cooperativite. 2002.

6. Manning PJ. The Biology of the Laboratory. 2014.

7. Fitzgerald Industries International. Rabbit Blood-Fitzgerald. 2016.

8. Lim H W G, Wortis M, Mukhopadhyay R. Stomatocyte-discocyte-echinocyte sequence of the human red blood cell: evidence for the bilayer- couple hypothesis from membrane mechanics. Proc Natl Acad Sci U S A. 2002;99(26):16766–9.

9. Gwo K. Ionizing radiation-induced structural modification of human red blood cells. 1991;45–52.

10. Ilesanmi OO. Sickle Cell Disease (SCD) and Stem Cell Therapy (SCT): Implications for Psychotherapy and Genetic Counselling in Africa. 2007;

11. Manwani D, Frenette PS. Vaso-occlusion in sickle cell disease : pathophysiology and novel targeted therapies. Hematology Am Soc Hematol Educ Program [Internet]. 2013;122(24):3892–8. Available from: http://www.ncbi.nlm.nih.gov/pubmed/24319205

12. Rees DC, Williams TN, Gladwin MT. Sickle-cell disease. Lancet [Internet]. Elsevier Ltd; 2010;376(9757):2018–31. Available from: http://dx.doi.org/10.1016/S0140-6736(10)61029-X

13. Gallik S. Osmosis-Cell Biology OLM. In 2011. Available from: cellbiologyolm.stevegallik.org

14. Walski T, Ludmi B, Chludzi N, Komorowska MB, Witkiewicz W. Individual Osmotic Fragility Distribution : A New Parameter for Determination of the Osmotic Properties of Human Red Blood Cells. 2014;2014.

15. Yamaji-Hasegawa A, Makino A, Baba T, Senoh Y, Kimura-Suda H, Sato SB, et al. Oligomerization and pore formation of a sphingomyelin-specific toxin, lysenin. Yamaji-Hasegawa, A, Makino, A, Baba, T, Senoh, Y, Kimura-Suda, H, Sato, S B, … Kobayashi, T (2003) Oligomerization pore Form a sphingomyelin-specific toxin, lysenin J Biol Chem 278(25), 22762–22770 http//doi.or. 2003;278(25):22762–70.

16. Aranda FJ, Teruel JA, Ortiz A. Further aspects on the hemolytic activity of the antibiotic lipopeptide iturin A. Biochim Biophys Acta - Biomembr. 2005;1713(1):51–6.

17. Arias M, Quijano JC, Haridas V, Gutterman JU, Lemeshko V V. Red blood cell

permeabilization by hypotonic treatments, saponin, and anticancer avicins. Biochim Biophys Acta - Biomembr [Internet]. Elsevier B.V.; 2010;1798(6):1189–96. Available from: http://dx.doi.org/10.1016/j.bbamem.2010.03.018

18. Mazzoni MC, Borgström P, Arfors KE, Intaglietta M. Dynamic fluid redistribution in hyperosmotic resuscitation of hypovolemic hemorrhage. Am J Physiol. 1988;255:H629–37.

19. Park Y, Best CA, Auth T, Gov NS, Safran SA, Popescu G, et al. Metabolic remodeling of the human red blood cell membrane. Pnas. 2010;107(4):1289–94.

20. Sprague RS, Hanson MS, Achilleus D, Bowles EA, Stephenson AH, Sridharan M, et al. Rabbit erythrocytes release ATP and dilate skeletal muscle arterioles in the presence of reduced oxygen tension. Pharmacol Reports. 2009;61(1):183–90.

21. da Cunha MML, Trepout S, Messaoudi C, Wu T-D, Ortega R, Guerquin-Kern J-L, et al. Overview of chemical imaging methods to address biological questions. Micron. 2016;84:23–36.

22. Wolf SG, Rez P, Kirchenbuechler D, Mutsafi Y, Horowitz B, Houben L, et al. Cryo-scanning transmission electron tomography of vitrified cells provides morphological and analytic information simultaneously. :2014.

23. da Cunha MML, Trepout S, Messaoudi C, Wu T Di, Ortega R, Guerquin-Kern JL, et al. Overview of chemical imaging methods to address biological questions. Vol. 84, Micron. 2016. p. 23–36.

24. Grandbois M, Dettmann W, Benoit M, Gaub HE. Affinity Imaging of Red Blood Cells Using an Atomic Force Microscope. J Histochem Cytochem. 2000;48(5):719–24.

25. Wood BR, Stoddart PR, McNaughton D. Molecular imaging of red blood cells by Raman spectroscopy. Aust J Chem. 2011;64(5):593–9.

26. Popescu G, Park Y, Choi W, Dasari RR, Feld MS, Badizadegan K. Imaging red blood cell dynamics by quantitative phase microscopy. Blood Cells, Mol Dis. 2008;41(1):10–6.

27. Thorn K. A quick guide to light microscopy in cell biology. Mol Biol Cell [Internet]. 2016;27(2):219–22. Available from: http://www.molbiolcell.org/content/27/2/219.full

28. Yamamoto Y, Shinohara K. Application of X-ray microscopy in analysis of living hydrated cells. Anat Rec. 2002;269(5):217–23.

29. Rajagopal Vadivambal DSJ. Bio-Imaging Principles, Techniques and Applications. 2015.

30. Maser J, Osanna A, Wang Y, Jacobsen C, Kirz J, Spector S, et al. Soft X-ray microscopy with a cryo scanning transmission X-ray microscope : I . Instrumentation , imaging and spectroscopy. 2000;197(January):68–79.

31. Kundu MR, White SM, Gopalswamy N, Lim J. Millimeter, Microwave, Hard X-Ray, and Soft X-Ray Observations of Energetic Electron Populations in Solar Flares [Internet]. Vol. 90, The Astrophysical Journal Suppl. Series. 1994. 599-610 p. Available from: papers2://publication/uuid/759BC09B-8890-456F-928D-D10B8654A2BE

32. Gianoncelli A, Vaccari L, Kourousias G, Cassese D, Bedolla DE, Kenig S, et al. Soft X-Ray Microscopy Radiation Damage On Fixed Cells Investigated With Synchrotron Radiation FTIR Microscopy. Sci Rep [Internet]. 2015;5(April):10250. Available from: http://www.pubmedcentral.nih.gov/articlerender.fcgi?artid=4431353&tool=pmcentrez&rend

ertype=abstract

33. Rodenburg JM, Hurst AC, Cullis AG, Dobson BR, Pfeiffer F, Bunk O, et al. Hard-X-ray lensless imaging of extended objects. Phys Rev Lett. 2007;98(3):1–4.

34. Nishino Y, Takahashi Y, Kubo H, Furukawa H, Yamauchi K, Maeshima K, et al. Nanostructure analysis by coherent hard X-ray diffraction. J Phys Conf Ser. 2009;186:12056.

35. Kundu MR, White SM, Gopalswamy N, Lim J. Millimeter , Microwave , Hard X – ray and Soft X – ray Observations of Energetic Electron Populations in Solar Flares. 1993;1–23.

36. Antunes A, Safatle AM V., Barros PSM, Morelhao SL. X-ray imaging in advanced studies of ophthalmic diseases. Med Phys [Internet]. 2006;33(7):2338. Available from: http://scitation.aip.org/content/aapm/journal/medphys/33/7/10.1118/1.2207135

37. josk-11-2-76.pdf.

38. xdb-new.pdf.

39. Materlik G, Rayment T, Stuart DI. Diamond Light Source: status and perspectives. Philos Trans A Math Phys Eng Sci [Internet]. 2015;373(2036). Available from: http://www.pubmedcentral.nih.gov/articlerender.fcgi?artid=4308985&tool=pmcentrez&rendertype=abstract

40. Munkegade N. An X-ray microscopy perspective on the effect of glutaraldehyde fixation on cells. 2005;218(May):185–92.

41. Osanna A. X-ray microscopy:preparations for studies of frozen hydrated specimens. 1996;

42. Pelka JB. Synchrotron Radiation in Biology and Medicine. 2008;114(2).

43. Zhang M-Q, Zhou L, Deng Q-F, Xie Y-Y, Xiao T-Q, Cao Y-Z, et al. Ultra-high-resolution 3D digitalized imaging of the cerebral angioarchitecture in rats using synchrotron radiation. Sci Rep [Internet]. 2015;5(February):14982. Available from: http://www.nature.com/doifinder/10.1038/srep14982\nhttp://www.ncbi.nlm.nih.gov/pubmed/26443231

44. Vartanyants I a, Mancuso a P, Singer a, Yefanov OM, Gulden J. Coherence measurements and coherent diffractive imaging at FLASH. J Phys B At Mol Opt Phys. 2010;43(19):194016.

45. Schroer CG, Kuhlmann M, Hunger MD, Günzler TF, Kurapova O, Feste S, et al. Nanofocusing parabolic refractive X-ray lenses. Appl Phys Lett [Internet]. 2003;82(9):1485–7. Available from: http://dx.doi.org/10.1063/1.1556960

46. Miao J, Sandberg RRL, Song C. Coherent X-Ray Diffraction Imaging. IEEE J Sel Top Quantum Electron [Internet]. 2012;18(1):399–410. Available from: http://ieeexplore.ieee.org/xpls/abs_all.jsp?arnumber=5773472

47. Miao J, Sayre D, Chapman HN. Phase retrieval from the magnitude of the Fourier transforms of nonperiodic objects. J Opt Soc Am A [Internet]. 1997;15(6):1662. Available from: http://www.opticsinfobase.org/abstract.cfm?URI=JOSAA-15-6-1662\npapers3://publication/doi/10.1364/JOSAA.15.001662

48. Whitehead LW, Williams GJ, Quiney HM, Vine DJ, Dilanian RA, Flewett S, et al. Diffractive imaging using partially coherent X rays. Phys Rev Lett. 2009;103(24):1–4.

49. Idorenko PAS. Single-shot ptychography. 2016;3(1).

50. Stachnik K. Ptychographical measurements of biological specimen. 2012;1–14.

51. Dierolf M, Menzel A, Thibault P, Schneider P, Kewish CM, Wepf R, et al. Ptychographic X-ray computed tomography at the nanoscale. Nature [Internet]. Nature Publishing Group; 2010;467(7314):436–9. Available from: http://dx.doi.org/10.1038/nature09419

52. Chapman HN, Barty A, Bogan MJ, Boutet S, Frank M, Hau-Riege SP, et al. Femtosecond diffractive imaging with a soft-X-ray free-electron laser. Nat Phys [Internet]. 2006;2(12):839–43. Available from: http://www.nature.com/doifinder/10.1038/nphys461

53. Zhang F, Peterson I, Vila-comamala J, Diaz A, Bean R, Chen B, et al. Translation position determination in ptychographic coherent diffraction imaging. 2013;21(11):13592–606.

54. Howells MR, Beetz T, Chapman HN, Cui C, Holton JM, Jacobsen CJ, et al. Journal of Electron Spectroscopy and An assessment of the resolution limitation due to radiation-damage in X-ray diffraction microscopy. 2009;170:4–12.

55. Howells MR, Beetz T, Chapman HN, Cui C, Holton JM, Jacobsen CJ, et al. Author ' s personal copy An assessment of the resolution limitation due to radiation-damage in X-ray diffraction microscopy.

56. Winey M, Meehl JB, O'Toole ET, Giddings TH. Conventional transmission electron microscopy. Mol Biol Cell [Internet]. 2014;25(3):319–23. Available from: http://www.ncbi.nlm.nih.gov/pubmed/24482357

57. Chang IYT, Joester D. Cryo-planing of frozen-hydrated samples using cryo triple ion gun milling (CryoTIGM^{TM}). J Struct Biol [Internet]. Elsevier Inc.; 2015;192(3):569–79. Available from: http://dx.doi.org/10.1016/j.jsb.2015.11.002

58. López O, López-Iglesias C, Cócera M, Walther P, Parra JL, De La Maza A. Influence of chemical and freezing fixation methods in the freeze-fracture of stratum corneum. J Struct Biol. 2004;146(3):302–9.

59. Dobro MJ, Melanson LA, Jensen GJ, McDowall AW. Plunge freezing for electron cryomicroscopy [Internet]. Vol. 481, Methods in Enzymology. Elsevier Masson SAS; 2010. 63-82 p. Available from: http://dx.doi.org/10.1016/S0076-6879(10)81003-1

60. Lee SJ, Ha H, Nam K-H. Measurement of red blood cell aggregation using X-ray phase contrast imaging. [Internet]. 5th ed. Vol. 18, Optics express. 2010. 26052-26061 p. Available from: http://www.ncbi.nlm.nih.gov/books/NBK21154/

61. Ly J, Marticorena R, Donnelly S. Red Blood Cell Survival in Chronic Renal Failure. 2004;44(4):715–9.

62. Khairy K, Foo J, Howard J. Shapes of Red Blood Cells: Comparison of 3D Confocal Images with the Bilayer-Couple Model. Cell Mol Bioeng. 2008;1(2–3):173–81.

9. APPENDIX

9.1 Detailed sketch of Red Blood Cells Sample Preparations

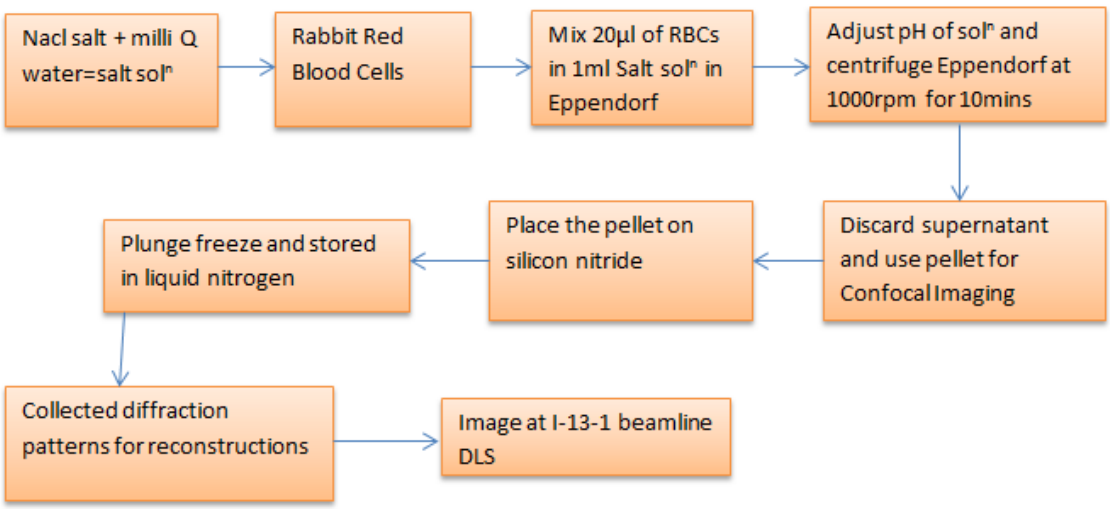

9.2 Cell Count

	Area	Mean	StdDev	Circ.	AR	Round	Solidity
1	0.007	255	0	0.637	1.505	0.665	0.764
2	2.17E-04	255	0	1	2	0.5	1
3	1.09E-04	255	0	1	1	1	1
4	1.09E-04	255	0	1	1	1	1
5	1.09E-04	255	0	1	1	1	1
6	1.09E-04	255	0	1	1	1	1
7	0.004	255	0	0.871	1.312	0.762	0.85
8	1.09E-04	255	0	1	1	1	1
9	1.09E-04	255	0	1	1	1	1
10	0.014	255	0	0.284	2.529	0.395	0.526
11	5.43E-04	255	0	0.462	3.678	0.272	0.667
12	1.09E-04	255	0	1	1	1	1
13	0.002	255	0	0.83	2.247	0.445	0.909
14	0.014	255	0	0.323	2.032	0.492	0.605
15	1.09E-04	255	0	1	1	1	1
16	3.26E-04	255	0	0.809	3	0.333	1
17	7.60E-04	255	0	0.8	1.73	0.578	0.737
18	0.001	255	0	0.776	1.399	0.715	0.741
19	1.09E-04	255	0	1	1	1	1

20	0.002	255	0	0.587	2.065	0.484	0.778
21	6.51E-04	255	0	0.809	2.237	0.447	0.857
22	2.17E-04	255	0	1	2	0.5	1
23	1.09E-04	255	0	1	1	1	1
24	0.003	255	0	0.543	1.644	0.608	0.688
25	0.002	255	0	0.857	1.91	0.523	0.821
26	3.26E-04	255	0	1	1.464	0.683	0.857
27	1.09E-04	255	0	1	1	1	1
28	0.013	255	0	0.563	1.625	0.616	0.78
29	0.003	255	0	0.714	1.82	0.55	0.781
30	1.09E-04	255	0	1	1	1	1
31	1.09E-04	255	0	1	1	1	1
32	3.26E-04	255	0	1	1.464	0.683	0.857
33	0.002	255	0	0.756	1.528	0.655	0.73
34	0.011	255	0	0.31	2.871	0.348	0.616
35	4.34E-04	255	0	0.857	1.468	0.681	0.8
36	0.011	255	0	0.63	1.691	0.591	0.795
37	0.003	255	0	0.819	2.115	0.473	0.862
38	3.26E-04	255	0	1	1.464	0.683	0.857
39	1.09E-04	255	0	1	1	1	1
40	4.34E-04	255	0	1	1	1	1
41	0.016	255	0	0.216	1.77	0.565	0.43
42	1.09E-04	255	0	1	1	1	1
43	1.09E-04	255	0	1	1	1	1
44	3.26E-04	255	0	0.643	2.702	0.37	0.667
45	2.17E-04	255	0	1	2	0.5	1
46	1.09E-04	255	0	1	1	1	1
47	2.17E-04	255	0	1	2	0.5	1
48	1.09E-04	255	0	1	1	1	1
49	1.09E-04	255	0	1	1	1	1
50	1.09E-04	255	0	1	1	1	1
51	3.26E-04	255	0	1	1.464	0.683	0.857
52	0.007	255	0	0.38	3.145	0.318	0.682
53	0.006	255	0	0.493	2.785	0.359	0.689
54	4.34E-04	255	0	1	1	1	1
55	3.26E-04	255	0	1	1.464	0.683	0.857
56	8.68E-04	255	0	0.52	1.643	0.609	0.615
57	0.002	255	0	0.82	1.768	0.566	0.739
58	6.51E-04	255	0	0.532	2.911	0.344	0.667
59	1.09E-04	255	0	1	1	1	1
60	0.027	255	0	0.182	1.086	0.921	0.509
61	3.26E-04	255	0	0.643	2.702	0.37	0.667
62	0.002	255	0	0.568	2.16	0.463	0.7
63	5.43E-04	255	0	0.873	1.496	0.668	0.714
64	0.002	255	0	1	1.248	0.801	0.947

65	8.68E-04	255	0	0.645	1.787	0.56	0.696
66	0.006	255	0	0.247	1.829	0.547	0.466
67	1.09E-04	255	0	1	1	1	1
68	2.17E-04	255	0	1	2	0.5	1
69	4.34E-04	255	0	0.857	2.031	0.492	0.8
70	8.68E-04	255	0	0.539	3.759	0.266	0.8
71	0.014	255	0	0.244	1.85	0.541	0.516
72	0.001	255	0	0.454	3.826	0.261	0.634
73	2.17E-04	255	0	1	2	0.5	1
74	0.014	255	0	0.206	2.362	0.423	0.534
75	0.001	255	0	0.601	2.394	0.418	0.765
76	0.004	255	0	0.497	2.351	0.425	0.714
77	2.17E-04	255	0	0.785	2.646	0.378	0.667
78	3.26E-04	255	0	1	1.464	0.683	0.857
79	1.09E-04	255	0	1	1	1	1
80	1.09E-04	255	0	1	1	1	1
81	2.17E-04	255	0	1	2	0.5	1
82	0.002	255	0	0.376	1.757	0.569	0.576
83	2.17E-04	255	0	1	2	0.5	1
84	0.004	255	0	0.77	1.526	0.655	0.808
85	0.001	255	0	1	1.45	0.69	0.897
86	0.001	255	0	0.715	1.781	0.562	0.846
87	1.09E-04	255	0	1	1	1	1
88	1.09E-04	255	0	1	1	1	1
89	0.003	255	0	0.572	1.77	0.565	0.738
90	8.68E-04	255	0	0.82	1.6	0.625	0.8
91	0.001	255	0	0.78	1.781	0.562	0.733
92	0.002	255	0	0.674	1.168	0.856	0.741
93	0.003	255	0	0.605	1.589	0.629	0.732
94	0.006	255	0	0.527	2.244	0.446	0.76
95	2.17E-04	255	0	1	2	0.5	1
96	0.001	255	0	1	1.551	0.645	0.909
97	3.26E-04	255	0	1	1.464	0.683	0.857
98	3.26E-04	255	0	0.643	2.702	0.37	0.667
99	0.577	255	0	0.02	1.384	0.722	0.316
100	0.005	255	0	0.528	2.572	0.389	0.696
101	1.09E-04	255	0	1	1	1	1
102	0.011	255	0	0.34	2.434	0.411	0.558
103	0.003	255	0	0.555	2.203	0.454	0.694
104	5.43E-04	255	0	0.873	2.188	0.457	0.714
105	1.09E-04	255	0	1	1	1	1
106	0.005	255	0	0.578	1.739	0.575	0.71
107	2.17E-04	255	0	1	2	0.5	1
108	0.004	255	0	0.594	1.809	0.553	0.686
109	0.004	255	0	0.672	1.628	0.614	0.756

110	0.005	255	0	0.524	2.839	0.352	0.773
111	0.001	255	0	0.659	2.738	0.365	0.786
112	0.002	255	0	0.976	1.287	0.777	0.857
113	5.43E-04	255	0	1	1.553	0.644	0.909
114	0.003	255	0	0.653	2.634	0.38	0.737
115	1.09E-04	255	0	1	1	1	1
116	0.329	255	0	0.021	2.275	0.44	0.25
117	0.005	255	0	0.715	1.416	0.706	0.772
118	2.17E-04	255	0	1	2	0.5	1
119	3.26E-04	255	0	0.643	2.702	0.37	0.667
120	0.002	255	0	0.629	1.266	0.79	0.8
121	2.17E-04	255	0	1	2	0.5	1
122	1.09E-04	255	0	1	1	1	1
123	2.17E-04	255	0	1	2	0.5	1
124	0.006	255	0	0.553	1.9	0.526	0.723
125	5.43E-04	255	0	1	1.553	0.644	0.909
126	7.60E-04	255	0	0.898	1.895	0.528	0.737
127	4.34E-04	255	0	0.645	4	0.25	1
128	2.17E-04	255	0	0.785	2.646	0.378	0.667
129	3.26E-04	255	0	1	1.464	0.683	0.857
130	5.43E-04	255	0	1	1.553	0.644	0.909
131	2.17E-04	255	0	1	2	0.5	1
132	0.002	255	0	0.723	1.998	0.501	0.772
133	0.006	255	0	0.506	3.073	0.325	0.686
134	2.17E-04	255	0	0.785	2.646	0.378	0.667
135	1.09E-04	255	0	1	1	1	1
136	2.17E-04	255	0	1	2	0.5	1
137	5.43E-04	255	0	0.873	1.882	0.531	0.714
138	0.005	255	0	0.496	2.808	0.356	0.676
139	4.34E-04	255	0	0.857	2	0.5	0.8
140	0.003	255	0	0.914	1.444	0.693	0.842
141	1.09E-04	255	0	1	1	1	1
142	0.003	255	0	0.641	1.587	0.63	0.781
143	3.26E-04	255	0	0.809	3	0.333	1
144	6.51E-04	255	0	1	1.291	0.775	0.8
145	2.17E-04	255	0	1	2	0.5	1
146	2.17E-04	255	0	1	2	0.5	1
147	1.09E-04	255	0	1	1	1	1
148	0.004	255	0	0.485	1.853	0.54	0.655
149	0.005	255	0	0.867	1.6	0.625	0.843
150	4.34E-04	255	0	0.857	1.468	0.681	0.8
151	0.006	255	0	0.535	2.022	0.495	0.732
152	1.09E-04	255	0	1	1	1	1
153	0.001	255	0	0.643	1.367	0.732	0.75
154	4.34E-04	255	0	1	2.031	0.492	0.8

155	0.025	255	0	0.153	3.648	0.274	0.475
156	0.003	255	0	0.667	2.177	0.459	0.767
157	2.17E-04	255	0	0.785	2.646	0.378	0.667
158	0.001	255	0	0.637	2.027	0.493	0.733
159	3.26E-04	255	0	1	1.464	0.683	0.857
160	4.34E-04	255	0	1	1	1	1
161	1.09E-04	255	0	1	1	1	1
162	1.09E-04	255	0	1	1	1	1
163	0.002	255	0	0.524	2.147	0.466	0.667
164	0.002	255	0	1	1.02	0.981	0.933
165	0.001	255	0	0.887	2.025	0.494	0.846
166	0.004	255	0	0.608	2.568	0.389	0.757
167	2.17E-04	255	0	1	2	0.5	1
168	3.26E-04	255	0	1	1.464	0.683	0.857
169	0.011	255	0	0.419	2.093	0.478	0.669
170	2.17E-04	255	0	1	2	0.5	1
171	1.09E-04	255	0	1	1	1	1
172	0.002	255	0	0.543	2.433	0.411	0.679
173	0.013	255	0	0.211	2.616	0.382	0.599
174	3.26E-04	255	0	1	1.464	0.683	0.857
175	4.34E-04	255	0	0.611	3.093	0.323	0.667
176	0.002	255	0	0.719	1.383	0.723	0.727
177	8.68E-04	255	0	0.914	1.195	0.837	0.8
178	6.51E-04	255	0	0.916	1.124	0.89	0.8
179	0.002	255	0	0.994	1.165	0.858	0.889
180	0.001	255	0	0.887	1.921	0.521	0.8
181	0.002	255	0	0.38	3.682	0.272	0.571
182	3.26E-04	255	0	1	1.464	0.683	0.857
183	1.09E-04	255	0	1	1	1	1
184	1.09E-04	255	0	1	1	1	1
185	0.007	255	0	0.385	2.337	0.428	0.67
186	1.09E-04	255	0	1	1	1	1
187	0.001	255	0	0.78	1.722	0.581	0.815
188	0.002	255	0	0.764	1.669	0.599	0.769
189	0.005	255	0	0.764	1.435	0.697	0.867
190	1.09E-04	255	0	1	1	1	1
191	6.51E-04	255	0	0.809	2.237	0.447	0.857
192	1.09E-04	255	0	1	1	1	1
193	2.17E-04	255	0	1	2	0.5	1
194	0.001	255	0	0.579	1.782	0.561	0.606
195	4.34E-04	255	0	0.698	2.654	0.377	0.667
196	0.002	255	0	0.993	1.31	0.763	0.848
197	1.09E-04	255	0	1	1	1	1
198	2.17E-04	255	0	1	2	0.5	1
199	0.005	255	0	0.547	1.24	0.806	0.706

200	0.057	255	0	0.091	1.561	0.641	0.514
201	9.77E-04	255	0	0.638	1.761	0.568	0.692
202	1.09E-04	255	0	1	1	1	1
203	2.17E-04	255	0	1	2	0.5	1
204	1.09E-04	255	0	1	1	1	1
205	3.26E-04	255	0	0.809	3	0.333	1
206	3.26E-04	255	0	1	1.464	0.683	0.857
207	0.008	255	0	0.373	1.286	0.777	0.635
208	1.09E-04	255	0	1	1	1	1
209	1.09E-04	255	0	1	1	1	1
210	0.001	255	0	1	1.148	0.871	0.897
211	0.003	255	0	0.829	1.164	0.859	0.806
212	0.006	255	0	0.476	1.958	0.511	0.648
213	0.005	255	0	0.543	2.433	0.411	0.734
214	1.09E-04	255	0	1	1	1	1
215	3.26E-04	255	0	1	1.464	0.683	0.857
216	0.01	255	0	0.29	1.779	0.562	0.56
217	1.09E-04	255	0	1	1	1	1
218	1.09E-04	255	0	1	1	1	1
219	2.17E-04	255	0	1	2	0.5	1
220	0.001	255	0	0.887	1.56	0.641	0.846
221	1.09E-04	255	0	1	1	1	1
222	1.09E-04	255	0	1	1	1	1
223	4.34E-04	255	0	0.857	2	0.5	0.8
224	1.09E-04	255	0	1	1	1	1
225	0.004	255	0	0.529	1.603	0.624	0.636
226	0.004	255	0	0.501	2.987	0.335	0.694
227	0.002	255	0	0.772	1.625	0.615	0.78
228	1.09E-04	255	0	1	1	1	1
229	0.003	255	0	0.564	1.416	0.706	0.727
230	1.09E-04	255	0	1	1	1	1
231	6.51E-04	255	0	0.686	2.335	0.428	0.75
232	2.17E-04	255	0	1	2	0.5	1
233	6.51E-04	255	0	1	1.291	0.775	0.8
234	1.09E-04	255	0	1	1	1	1
235	0.001	255	0	1	1.551	0.645	0.929
236	0.003	255	0	0.319	1.993	0.502	0.544
237	0.016	255	0	0.359	2.891	0.346	0.677
238	5.43E-04	255	0	0.572	3.145	0.318	0.667
239	4.34E-04	255	0	0.645	4	0.25	1
240	0.002	255	0	0.712	1.436	0.696	0.793
241	1.09E-04	255	0	1	1	1	1
242	1.09E-04	255	0	1	1	1	1
243	0.006	255	0	0.635	1.728	0.579	0.752
244	1.09E-04	255	0	1	1	1	1

245	0.01	255	0	0.363	2.498	0.4	0.648
246	2.17E-04	255	0	1	2	0.5	1
247	4.34E-04	255	0	1	1.468	0.681	0.8
248	0.002	255	0	0.802	1.194	0.837	0.808
249	2.17E-04	255	0	1	2	0.5	1
250	7.60E-04	255	0	0.621	3.002	0.333	0.667
251	0.003	255	0	0.679	1.599	0.625	0.833
252	1.09E-04	255	0	1	1	1	1
253	1.09E-04	255	0	1	1	1	1
254	0.004	255	0	0.81	1.616	0.619	0.84
255	0.011	255	0	0.322	2.932	0.341	0.585
256	0.001	255	0	0.715	1.569	0.637	0.786
257	0.003	255	0	0.365	2.868	0.349	0.66
258	1.09E-04	255	0	1	1	1	1
259	4.34E-04	255	0	0.857	1.468	0.681	0.8
260	1.09E-04	255	0	1	1	1	1
261	0.005	255	0	0.726	2.025	0.494	0.848
262	0.013	255	0	0.509	1.377	0.726	0.786
263	0.005	255	0	0.829	1.524	0.656	0.85
264	1.09E-04	255	0	1	1	1	1
265	1.09E-04	255	0	1	1	1	1
266	0.001	255	0	0.982	1.028	0.973	0.769
267	2.17E-04	255	0	1	2	0.5	1
268	0.008	255	0	0.566	2.382	0.42	0.74
269	0.007	255	0	0.397	1.786	0.56	0.61
270	3.26E-04	255	0	1	1.464	0.683	0.857
271	0.002	255	0	0.454	2.914	0.343	0.6
272	3.26E-04	255	0	1	1.464	0.683	0.857
273	1.09E-04	255	0	1	1	1	1
274	1.09E-04	255	0	1	1	1	1
275	0.013	255	0	0.272	1.721	0.581	0.571
276	0.007	255	0	0.417	2.632	0.38	0.727
277	2.17E-04	255	0	1	2	0.5	1
278	1.09E-04	255	0	1	1	1	1
279	1.09E-04	255	0	1	1	1	1
280	0.004	255	0	0.428	1.602	0.624	0.64
281	0.005	255	0	0.572	2.642	0.379	0.808
282	1.09E-04	255	0	1	1	1	1
283	1.09E-04	255	0	1	1	1	1
284	9.77E-04	255	0	0.799	2.239	0.447	0.75
285	8.68E-04	255	0	0.588	3.759	0.266	0.8
286	1.09E-04	255	0	1	1	1	1
287	1.09E-04	255	0	1	1	1	1
288	0.003	255	0	0.793	1.055	0.948	0.789
289	3.26E-04	255	0	1	1.464	0.683	0.857

290	1.09E-04	255	0	1	1	1	1
291	0.002	255	0	0.75	2.139	0.468	0.778
292	0.001	255	0	0.982	1.316	0.76	0.769
293	1.09E-04	255	0	1	1	1	1
294	0.003	255	0	0.439	1.262	0.792	0.701
295	0.005	255	0	0.633	2.179	0.459	0.789
296	1.09E-04	255	0	1	1	1	1
297	0.002	255	0	0.786	2.049	0.488	0.944
298	1.09E-04	255	0	1	1	1	1
299	2.17E-04	255	0	1	2	0.5	1
300	0.004	255	0	0.705	1.531	0.653	0.745
301	3.26E-04	255	0	0.524	1.567	0.638	0.6
302	1.09E-04	255	0	1	1	1	1
303	0.001	255	0	0.781	2.022	0.495	0.774
304	2.17E-04	255	0	1	2	0.5	1
305	2.17E-04	255	0	1	2	0.5	1
306	1.09E-04	255	0	1	1	1	1
307	0.002	255	0	0.796	1.448	0.691	0.844
308	0.002	255	0	0.863	1.861	0.537	0.898
309	2.17E-04	255	0	1	2	0.5	1
310	1.09E-04	255	0	1	1	1	1
311	0.001	255	0	0.922	1.416	0.706	0.812
312	1.09E-04	255	0	1	1	1	1
313	3.26E-04	255	0	0.754	2.702	0.37	0.667
314	9.77E-04	255	0	1	1.536	0.651	0.857
315	0.009	255	0	0.531	2.583	0.387	0.705
316	2.17E-04	255	0	1	2	0.5	1
317	4.34E-04	255	0	0.645	4	0.25	1
318	1.09E-04	255	0	1	1	1	1
319	3.26E-04	255	0	1	1.464	0.683	0.857
320	1.09E-04	255	0	1	1	1	1
321	3.26E-04	255	0	1	1.464	0.683	0.857
322	2.17E-04	255	0	1	2	0.5	1
323	1.09E-04	255	0	1	1	1	1
324	1.09E-04	255	0	1	1	1	1
325	2.17E-04	255	0	1	2	0.5	1
326	2.17E-04	255	0	1	2	0.5	1
327	2.17E-04	255	0	1	2	0.5	1
328	3.26E-04	255	0	1	1.464	0.683	0.857
329	1.09E-04	255	0	1	1	1	1
330	2.17E-04	255	0	1	2	0.5	1
331	1.09E-04	255	0	1	1	1	1
332	1.09E-04	255	0	1	1	1	1
333	1.09E-04	255	0	1	1	1	1
334	5.43E-04	255	0	0.873	1.496	0.668	0.714

335	1.09E-04	255	0	1	1	1	1
336	1.09E-04	255	0	1	1	1	1
337	1.09E-04	255	0	1	1	1	1
338	1.09E-04	255	0	1	1	1	1
339	1.09E-04	255	0	1	1	1	1